Sains Malaysiana 54(4)(2025): 1187-1207
http://doi.org/10.17576/jsm-2025-5404-18

Optimising Variable Sample Size $\bar{X}$ Chart through Median Run Length with Estimated Process Parameters

(Pengoptimuman Carta $\bar{X}$bar Bersaiz Sampel Berubah-ubah melalui Panjang Larian Median dengan Parameter Proses Anggaran)

WEI LIN TEOH[1,2,*], KAI LE GOH[1], ZHI LIN CHONG[3], XINYING CHEW[4], MING HA LEE[5] & KHAI WAH KHAW[6]

[1]School of Mathematical and Computer Sciences, Heriot-Watt University Malaysia, 62200 Putrajaya, Malaysia
[2]International Chair in Data Science & Explainable Artificial Intelligence, International Research Institute for Artificial Intelligence and Data Science, Dong A University, Danang, Vietnam
[3]Department of Electronic Engineering, Faculty of Engineering and Green Technology, Universiti Tunku Abdul Rahman, 31900 Kampar, Perak, Malaysia
[4]School of Computer Science, Universiti Sains Malaysia, 11800 Gelugor, Pulau Pinang, Malaysia
[5]Faculty of Engineering, Computing and Science, Swinburne University of Technology Sarawak Campus, 93350 Kuching, Sarawak, Malaysia
[6]School of Management, Universiti Sains Malaysia, 11800 Gelugor, Pulau Pinang, Malaysia

Received: 30 August 2024/Accepted: 18 December 2024

ABSTRACT

The classic charting procedures for designing the estimated process parameters-based variable sample size (VSS) $\bar{X}$ chart rely on the average run length (ARL) criterion. Nevertheless, variations in the number of Phase-I samples and sample size, as well as the magnitude of the process mean shift affect the skewness of the run-length distribution for a control chart. Hence, we claim that the ARL can be a misleading metric when adopted in the estimated process parameters-based control charts. Instead, examining percentiles of the run-length distribution, which focus on the run-length behaviour, are more realistic and intuitive. From this point of view, this paper aims to develop two new optimal VSS $\bar{X}$ charts using estimated process parameters, by minimising the (i) median run length (MRL) and (ii) expected MRL criteria, for known and unknown shift-size cases, respectively. Besides, the 5th and 95th percentiles are computed to closely examine the variability of the run length. In this paper, two VSS schemes that involve estimated process parameters are investigated extensively, i.e., the first sample size can be either small or large. Various practically manageable Phase-I sample sizes and magnitudes of process mean shift are implemented in the optimal design of the proposed charts. The results ascertain that the proposed optimal VSS $\bar{X}$ charts based on estimated process parameters not only provide a comprehensible interpretation for quality practitioners, but also give a low false-alarm rate. The proposed optimal charts are illustrated using real data from a wafer substrate manufacturing company.

Keywords: median run length; optimal design; percentile of the run-length distribution; process parameter estimation; variable sample size $\bar{X}$ chart

ABSTRAK

Prosedur carta klasik untuk mereka carta $\bar{X}$ bersaiz sampel berubah-ubah (VSS) berdasarkan anggaran parameter proses adalah bergantung pada kriteria panjang larian purata (ARL). Namun begitu, variasi dalam bilangan sampel Fasa-I dan saiz sampel, serta magnitud anjakan purata proses mempengaruhi kepencongan taburan panjang larian untuk carta kawalan. Oleh itu, kami berpendapat bahawa ARL merupakan metrik yang mengelirukan apabila digunakan dalam carta kawalan berdasarkan parameter proses yang dianggarkan. Sebaliknya, pemeriksaan percentil taburan panjang larian yang memberi tumpuan kepada tingkah laku panjang larian adalah lebih realistik dan intuitif. Dari sudut pandangan ini, kajian ini bertujuan untuk mencipta dua reka bentuk optimum baharu bagi carta VSS $\bar{X}$ berdasarkan parameter proses yang dianggarkan dengan meminimumkan kriteria masing-masing untuk (i) panjang larian median (MRL) dan (ii) jangkaan MRL untuk kes perubahan saiz anjakan yang diketahui dan tidak diketahui. Selain itu, percentil ke-5 dan ke-95 dikira dengan teliti untuk mengukur variabiliti dalam panjang larian. Dalam kajian ini, dua skim VSS yang melibatkan parameter proses yang dianggarkan dikaji dengan secara mendalam, iaitu, saiz sampel pertama adalah sama dengan kecil atau besar. Pelbagai saiz sampel Fasa-I yang mudah diurus dan magnitud anjakan purata proses digunakan dalam reka bentuk optimum carta yang dicadangkan. Hasil kajian kami menunjukkan bahawa carta VSS $\bar{X}$ optimum yang dicadangkan berdasarkan parameter proses yang dianggarkan bukan sahaja memberikan tafsiran yang komprehensif kepada pengamal kualiti, tetapi juga memberikan kadar amaran palsu yang rendah. Carta optimum yang dicadangkan diilustrasikan dengan menggunakan data sebenar daripada sebuah syarikat pembuatan substrat wafer.

Kata kunci: Anggaran proses parameter; carta $\bar{X}$ bersaiz sampel berubah-ubah; panjang larian median; reka bentuk optimum; taburan peratusan panjang larian

INTRODUCTION

Quality control charts, a fundamental technique in statistical process control (SPC), serve as powerful tools for the real-time monitoring of processes. They are widely adopted to ascertain if a production process is operating in a stable and statistically controlled state. In practical applications, process parameters are hardly known with absolute certainty. Typically, process monitoring involves two distinct phases, which are Phase-I and Phase-II. During the Phase-I analysis, quality control charts are employed comprehensively to evaluate the process stability and capability. From the stable Phase-I process data, the in-control process parameters, i.e., μ_0 and σ_0, which indicate the population mean and standard deviation, respectively, are estimated. Phase-II analysis employs control charts to continuously monitor the process as new data are collected successively over time, facilitating the identification of any process changes during this prospective monitoring.

In most situations, practitioners seek to estimate μ_0 and σ_0 from a small set of Phase-I samples, so that the subsequent process monitoring can commence promptly in the Phase-II stage. However, as discussed by several SPC scholars (Chong et al. 2024; Shepherd, Champ & Rigdon 2016), employing a small set of Phase-I samples for process parameters estimation can significantly impact the functionality and capability of control charts. To circumvent this issue, an increasing effort is being placed on developing new control charting parameters for the quality control charts that incorporate estimated process parameters. Some of the works include the variable sample size (VSS) $\bar{X}$ chart (Castagliola, Maravelakis & Figueiredo 2012), the double sampling (DS) $\bar{X}$ chart (Teoh et al. 2015), the exponentially weighted moving average (EWMA) median chart (Castagliola et al. 2016), the triple sampling $\bar{X}$ chart (Mim et al. 2022), and the sequential probability ratio test (SPRT) chart (Teoh et al. 2024). Jensen et al. (2006) hypothesised that process parameter estimation substantially influences the control charts using VSS and variable sampling interval (VSI) schemes due to their enhanced sensitivity to small shifts. In the VSS chart, the sample size (n) can be adjusted across different levels, with the control-limit coefficient and sampling interval remaining unchanged. Compared to the VSI with fixed time $\bar{X}$ chart, Reynolds (1996) claimed that significant improvements are achieved for the VSS $\bar{X}$ chart for identifying small levels of shifts in process mean. Lately, the VSS run sum (RS) chart, introduced by Yeong et al. (2022), offers an enhanced approach for monitoring the coefficient of variation (CV). The VSS RS chart surpasses the traditional RS CV chart and demonstrates effectiveness in monitoring the weights of discarded zinc alloy material. Moreover, Lim et al. (2024) developed the VSS side-sensitive synthetic CV control chart, which establishes superior performance relative to the VSS RS and VSS EWMA CV charts, particularly in the case of moderate to large levels of process shift sizes. This chart also shows efficiency in tracking the sintering process in manufacturing environments. Given the benefits and widespread industrial applications of VSS-type charts, this paper explores the estimated process parameters-based VSS $\bar{X}$ chart.

Among current SPC studies, there is an overemphasis on the average run length (ARL) as the primary performance and design indicator for control charts that use estimated process parameters. Focusing solely on the ARL measure is detrimental and not meaningful, especially for control charts using estimated process parameters (Teoh et al. 2014; Epprecht, Loureiro & Chakraborti 2015; Lee et al. 2023). This paper extensively shows that the shape and skewness of the run-length distribution for the VSS $\bar{X}$ chart using estimated process parameters, alter with the number of Phase-I samples m and sample sizes n, as well as the magnitude of shift sizes δ. Also, findings in Section 3 of this paper indicate that the ARL-based VSS $\bar{X}$ chart when using estimated process parameters exhibits high false alarm rates. Undoubtedly, this degraded chart performance will affect practitioners' confidence. Looking at these arising problems, it is a high time that the alternative chart design criterion needs to be proposed for the VSS $\bar{X}$ chart that involves estimated process parameters. Numerous SPC scholars, namely Chakraborti (2007), Chong et al. (2022), Karimi et al. (2023), and Zhou et al. (2012) have argued that percentiles of the run-length distribution offer practitioners more practical advantages as they deliver useful and essential insights into the actual and expected run length (RL) behaviour. Along this line, the median run length (MRL), i.e., the 50th percentile of the run-length distribution, often proves to be a fair choice for representing central tendency (Teh et al. 2015). The reason is that, in right-skewed distributions, the median usually falls below the mean. Additionally, because of its robustness property, the median is considerably less influenced by outliers. With these advantages as motivation, Teoh et al. (2016), You et al. (2016), Gao et al. (2019), and Qiao et al. (2022), have recommended using the MRL criterion as the key performance and design metric for control charts.

Since the MRL provides a more useful piece of information compared to the ARL, it is used as an alternative design criterion for the VSS $\bar{X}$ chart that uses estimated process parameters. In real-life scenarios, it is uncommon to have precise knowledge of both process parameters and future process changes. Given these issues, an analysis of control charts methodologies that involves estimated process parameters for unknown shift-size conditions is vitally viewed. Therefore, this paper proposes two new optimal statistical designs for the VSS $\bar{X}$ chart using estimated process parameters, i.e., by minimising (i) the out-of-control MRL (MRL_1) and (ii) the out-of-control expected MRL (EMRL) metrics, for known and unknown shift-size cases, respectively. Note that optimisation frameworks and algorithms for the VSS $\bar{X}$ chart, focused on estimated process parameters and minimising the out-of-control ARL (ARL_1) was discussed by Castagliola et al. (2012). However, they only explore a single VSS scheme, i.e., the predefined first subgroup (n_1) is the small sample size (n_S). The added merit of this paper is that we consider two VSS schemes for the VSS $\bar{X}$ chart using estimated process parameters. These two VSS schemes include $n_1 = n_S$ and $n_1 = n_L$, with n_L denoting the larger sample size and $n_S < n_L$. Note that selecting $n_1 = n_S$ (i.e., small sample size for the first subgroup) allows the chart to maintain efficiency during the initial stage of process monitoring, while choosing $n_1 = n_L$ (i.e., large sample size for the first subgroup) provides a stronger foundation to enhance the early identification of large shifts in the process. This $n_1 = n_L$ feature is similar to the fast initial response in control charts, where a larger initial sample size enhances the ability to detect significant shifts.

This paper is arranged in the following sequence. First, we outline the properties of the RL for the VSS $\bar{X}$ chart using estimated process parameters. Next, we conduct performance evaluations for the VSS $\bar{X}$ chart using estimated process parameters based on the ARL metric. We then develop MRL and EMRL optimisation algorithms for the VSS $\bar{X}$ charts using estimated process parameters. Afterwards, the proposed optimal VSS $\bar{X}$ chart using estimated process parameters, is applied to real-life data from a wafer manufacturing company. Last, this paper ends with some concluding remarks.

THE VSS $\bar{X}$ CHART USING ESTIMATED PROCESS PARAMETERS

The main discussion of this section focuses on the VSS $\bar{X}$ chart using estimated process parameters. Readers can seek information on the construction of the VSS $\bar{X}$ chart using known process parameters from Teoh et al. (2017). In practice, the μ_0 and σ_0 are often estimated using Phase-I data as both parameters are unknown. In the Phase-I data, m distinct samples are collected, each sample containing n individual observations, which are denoted as $\{X_{i,1}, X_{i,2}, \ldots, X_{i,n}\}$, where $i = 1, 2, \ldots, m$. We assume $X_{i,j}$, for $j = 1, 2, \ldots, n$, as being independent within each sample and across samples, and following a normal distribution, i.e., $X_{i,j} \sim N(\mu_0, \sigma_0^2)$. In this context, μ_0 and σ_0^2 denotes the in-control mean and variance, respectively. The grand mean, often denoted as $\hat{\mu}_0$, is a frequently employed estimator for μ_0. This estimator is calculated using the formula

$$\hat{\mu}_0 = \frac{1}{m} \sum_{i=1}^{m} \bar{X}_i, \tag{1}$$

where $\bar{X}_i = \sum_{j=1}^{n} X_{i,j} / n$ represents the mean of the i^{th} sample for the Phase-I data. In the estimation of σ_0, the pooled estimator $\hat{\sigma}_0$ is widely adopted, which is given as

$$\hat{\sigma}_0 = \sqrt{\frac{1}{m(n-1)} \sum_{i=1}^{m} \sum_{j=1}^{n} \left(X_{i,j} - \bar{X}_i\right)^2}. \tag{2}$$

Let $\{Y_{i,1}, Y_{i,2}, \ldots, Y_{i,n_i}\}$, for $i = 1, 2, \ldots$, represents the quality characteristic taken from the Phase-II process. Assume that $Y_{i,j}$, for $j = 1, 2, \ldots, n_i$, and $n_i \in \{n_S, n_L\}$, is independent and normally distributed, i.e., $Y_{i,j} \sim N(\hat{\mu}_0, \hat{\sigma}_0^2)$. Hence, the plotting statistic ($\hat{Z}_i$) associated with the i^{th} sample corresponds to

$$\hat{Z}_i = \frac{(\bar{Y}_i - \hat{\mu}_0)\sqrt{n_i}}{\hat{\sigma}_0}, \tag{3}$$

where $\bar{Y}_i = \left(\sum_{j=1}^{n} Y_{i,j}\right)/n_i$. Let δ be the standardised mean shift size. When $\delta = 0$, the process is considered statistically in-control, conversely, if $\delta \neq 0$, it is deemed statistically out-of-control. By definition, $\hat{Z}_i \sim N(\delta\sqrt{n_i}, 1)$. Note that $\hat{Z}_i$ conforms to a standard normal $N(0, 1)$ distribution if $\delta = 0$. Note that the selection of $n_i \in \{n_S, n_L\}$ in Equation (3) demonstrates the adaptability of the VSS mechanism. Specifically, n_S is utilised under stable conditions to ensure efficiency, while n_L is employed when increased sensitivity to shifts is required.

Figure 1 shows the schematic representation of the operation for the VSS $\bar{X}$ chart. From Figure 1, the VSS $\bar{X}$ chart is partitioned into the central region ($I_S \in [-W, W]$), the warning region ($I_L \in [-K, -W) \cup (W, K]$), and the out-of-control region $I_{ooc} = (-\infty, -K) \cup (K, \infty)$. The VSS $\bar{X}$ chart operates through the following procedures:

Step 1 Calculate the control limits of W and K.

Step 2 Draw a random sample with size n_i and determine the sample statistic, $\hat{Z}_i$ as in Equation (3).

Step 3 Deduce that the process is in a statistically in-control condition if $\hat{Z}_i \in I_S$, thus, collect $n_{i+1} = n_S$ for the next sample.

Step 4 Deduce that the process continues to be statistically in-control if $\hat{Z}_i \in I_L$, thus, collect $n_{i+1} = n_L$ for the next sample to reinforce control.

Step 5 Generate an out-of-control status if $\hat{Z}_i \in I_{ooc}$, then, search and omit potential assignable causes.

As detailed by Costa (1994), the matrix $\hat{\mathbf{Q}}$ of transient probabilities for the VSS $\bar{X}$ chart can be obtained through the 3×3 transition probability matrix $\mathbf{P}$ as described below:

$$\mathbf{P} = \begin{pmatrix} \hat{\mathbf{Q}} & \hat{\mathbf{r}} \\ \mathbf{0}^T & 1 \end{pmatrix} = \begin{pmatrix} \hat{p}_S(n_S) & \hat{p}_L(n_S) & 1 - \hat{p}_S(n_S) - \hat{p}_L(n_S) \\ \hat{p}_S(n_L) & \hat{p}_L(n_L) & 1 - \hat{p}_S(n_L) - \hat{p}_L(n_L) \\ 0 & 0 & 1 \end{pmatrix}, \tag{4}$$

where $\mathbf{0} = (0, 0)^T$. Note that in matrix $\mathbf{P}$, the initial two states are considered as transient states, whereas the third

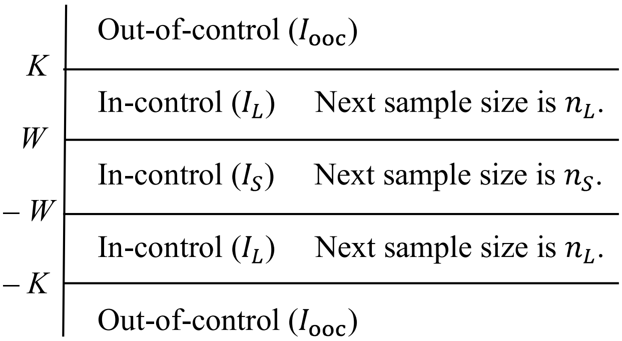

FIGURE 1. Schematic representation of the VSS $\bar{X}$ chart's operation

state is identified as an absorbing state. The conditional probabilities $\hat{p}_S(n_i)$ and $\hat{p}_L(n_i)$ for $n_i \in \{n_S, n_L\}$ in Equation (4) are formulated as (Castagliola et al. 2012)

$$\begin{aligned}\hat{p}_S(n_i) &= P\left(\hat{Z}_i \in I_S \middle| n_i, \hat{\mu}_0, \hat{\sigma}_0\right)\\ &= \Phi\left(U\sqrt{\frac{n_i}{mn}} + VW - \delta\sqrt{n_i}\right) - \Phi\left(U\sqrt{\frac{n_i}{mn}} - VW - \delta\sqrt{n_i}\right),\end{aligned} \quad (5)$$

and

$$\begin{aligned}\hat{p}_L(n_i) &= P\left(\hat{Z}_i \in I_L \middle| n_i, \hat{\mu}_0, \hat{\sigma}_0\right)\\ &= \Phi\left(U\sqrt{\frac{n_i}{mn}} - VW - \delta\sqrt{n_i}\right) - \Phi\left(U\sqrt{\frac{n_i}{mn}} - VK - \delta\sqrt{n_i}\right) + \Phi\left(U\sqrt{\frac{n_i}{mn}} + VK - \delta\sqrt{n_i}\right)\\ &\quad - \Phi\left(U\sqrt{\frac{n_i}{mn}} + VW - \delta\sqrt{n_i}\right),\end{aligned} \quad (6)$$

respectively, where $\Phi(\cdot)$ represents the cdf for the standard normal distribution. In Equations (5) and (6), the random variables U and V are specified as $U = (\hat{\mu}_0 - \mu_0)\sqrt{mn}/\sigma_0$ and $V = \hat{\sigma}_0/\sigma_0$, respectively. Since $\hat{\mu}_0 \sim N[\mu_0, \sigma_0^2/(mn)]$, then $U \sim N(0,1)$. Thus, the probability density function (pdf) of U, denoted as $f_U(u)$ is given by $f_U(u) = \phi(u)$. Here, $\phi(\cdot)$ signifies the pdf associated with the standard normal distribution. Since the random variable $V^2 = \hat{\sigma}_0^2/\sigma_0^2 \sim \gamma[m(n-1)/2, 2/[m(n-1)]]$ follows a gamma distribution with parameters $[m(n-1)]/2$ and $2/[m(n-1)]$, the pdf of V, $f_V(v)$ equals to $f_V(V) = 2V f_\gamma(v^2|m(n-1)/2, 2/[m(n-1)])$, where f_γ denotes the pdf of the gamma distribution.

The RL represents the number of samples that is required by a control chart to produce the first out-of-control point. When $\hat{\mu}_0$ and σ_0 are unknown, the unconditional run-length distribution is obtained by averaging the run-length distribution across all the feasible values of $\hat{\mu}_0$ and $\hat{\sigma}_0$. With the use of the conditional approach, we can derive formulae for the unconditional probability mass function (pmf), $f_{\mathrm{RL}}(\ell)$ and the cumulative distribution function (cdf), $F_{\mathrm{RL}}(\ell)$ for the VSS $\bar{X}$ chart based on estimated process parameters as follows:

$$f_{\mathrm{RL}}(\ell) = \int_{-\infty}^{+\infty}\int_0^{+\infty}\left(\mathbf{q}^T\hat{\mathbf{Q}}^{\ell-1}\hat{\mathbf{r}}\right)f_U(u)f_V(v)\,dv\,du \quad (7)$$

and

$$\begin{aligned}F_{\mathrm{RL}}(\ell) &= P(\mathrm{RL} \le \ell)\\ &= 1 - \int_{-\infty}^{+\infty}\int_0^{+\infty}\left(\mathbf{q}^T\hat{\mathbf{Q}}^{\ell-1}\mathbf{1}\right)f_U(u)f_V(v)\,dv\,du,\end{aligned} \quad (8)$$

respectively. Here, $\ell \in \{1, 2, 3, \ldots\}$, $\mathbf{q}$ denotes the 2×1 initial probability vector, $\hat{\mathbf{Q}}$ represents the 2×2 transition probability matrix, and $\hat{\mathbf{r}}$ is the 2×1 vector satisfying $\hat{\mathbf{r}} = \mathbf{1} - \hat{\mathbf{Q}}\mathbf{1}$, where $\mathbf{1}$ corresponds to a 2×1 vector with both entries equal to one. Note that $\mathbf{q} = (1, 0)^T$ if $n_1 = n_S$, while $\mathbf{q} = (0, 1)^T$ if $n_1 = n_L$. Note that $f_U(u)$ and $f_V(v)$ in Equations (7) and (8) follow the same definition as defined in the previous paragraph.

As defined by Gan (1993), the value ℓ_ϵ, for $0 < \epsilon < 1$, corresponds to the $(100\epsilon)^{\text{th}}$ percentiles of the run-length distribution, in which

$$P(\mathrm{RL} \le \ell_\epsilon - 1) \le \epsilon \text{ and } P(\mathrm{RL} \le \ell_\epsilon) > \epsilon. \quad (9)$$

Both Equations (8) and (9) are then utilised to evaluate the percentiles of the run-length distribution for the VSS $\bar{X}$ chart. To determine the MRL value, we set $\epsilon = 0.5$ in Equation (9), which corresponds to the 50th percentile of the run-length distribution.

For situations involving estimated process parameters, the mathematical expressions of the unconditional average sample size (ASS), ARL, and standard deviation of the run length (SDRL), for the VSS $\bar{X}$ chart are determined from

$$\mathrm{ASS} = \int_{-\infty}^{+\infty}\int_0^{+\infty}(n_S, n_L, n_1)\hat{\mathbf{R}}^{-1}\begin{pmatrix}\mathbf{q}\\0\end{pmatrix}f_U(u)f_V(v)\,dv\,du, \quad (10)$$

$$\mathrm{ARL} = \int_{-\infty}^{+\infty}\int_0^{+\infty}\mathbf{q}^T\left(\mathbf{I} - \hat{\mathbf{Q}}\right)^{-1}\mathbf{1}f_U(u)f_V(v)\,dv\,du, \quad (11)$$

and

$$\mathrm{SDRL} = \sqrt{\int_{-\infty}^{+\infty}\int_0^{+\infty}\left[2\mathbf{q}^T(\mathbf{I} - \mathbf{Q})^{-2}\hat{\mathbf{Q}}\mathbf{1} + \mathbf{q}^T\left(\mathbf{I} - \hat{\mathbf{Q}}\right)^{-1}\mathbf{1}\right]f_U(u)f_V(v)\,dv\,du - \mathrm{ARL}^2}, \quad (12)$$

respectively. $\mathbf{I}$ in Equations (11) and (12), is the 2×2 identity matrix. Note that the ASS in Equation (10) is defined based on the assumption of a process operating throughout an infinite time period. If $n_1 = n_S$, the 3 × 3 matrix $\hat{\mathbf{R}}$ in Equation (10) is obtained as

$$\hat{\mathbf{R}} = \begin{pmatrix} 1 & 1 & 1 \\ \hat{p}_L(n_S) & \hat{p}_L(n_L) - 1 & 0 \\ 1 - \hat{p}_S(n_S) - \hat{p}_L(n_S) & 1 - \hat{p}_S(n_L) - \hat{p}_L(n_L) & -1 \end{pmatrix}, \quad (13)$$

while if $n_1 = n_L$, $\hat{\mathbf{R}}$ is given as

$$\hat{\mathbf{R}} = \begin{pmatrix} \hat{p}_S(n_S) - 1 & \hat{p}_S(n_L) & 0 \\ 1 & 1 & 1 \\ 1 - \hat{p}_S(n_S) - \hat{p}_L(n_S) & 1 - \hat{p}_S(n_L) - \hat{p}_L(n_L) & -1 \end{pmatrix}. \quad (14)$$

PERFORMANCE EVALUATION OF THE ARL-BASED VSS $\bar{X}$ CHART USING ESTIMATED PROCESS PARAMETERS

Traditionally, the ARL has been employed as a primary performance measure for control charts that incorporate estimated process parameters. However, there are two key concerns associated with relying solely on the ARL (Montgomery 2013). The first concern is the very large value of the SDRL. The second concern is the highly skewed run-length distribution. Castagliola et al. (2012) developed the optimal ARL-based VSS $\bar{X}$ chart that involves estimated process parameters, which produces a satisfactory in-control ARL (ARL_0) value. However, the resulting values of in-control SDRL ($SDRL_0$) and out-of-control SDRL ($SDRL_1$) are quite large compared to their corresponding values of ARL_0 and out-of-control ARL (ARL_1), respectively. Such a situation is unfavourable. Therefore, this section draws the attention of practitioners towards the arising problems of the optimal design for the VSS $\bar{X}$ chart, especially when using the ARL metric with estimated process parameters.

Table 1 shows the ARLs, SDRLs, and the 5th ($\ell_{0.05}$), 25th ($\ell_{0.25}$), 50th (MRL), 75th ($\ell_{0.75}$), and 95th ($\ell_{0.95}$) percentiles of the run-length distribution for the ARL optimised VSS $\bar{X}$ chart when $n_1 = n_S$. Table 1 also examines multiple compositions of m, n, and δ. In the upper portion of Table 1, the optimal parameters (n_S, n_L, W, K) of the VSS $\bar{X}$ chart are provided for scenarios with both estimated ($m \in \{10, 20, 40, 80\}$) and known ($m = +\infty$) process parameters. These optimal parameters are obtained by minimising the ARL_1 ($\delta_{\text{opt}} = 1.0$) under the constraints of $ARL_0 = 370$ and $ASS_0 = \{3, 5\}$, where ASS_0 represents the in-control ASS. Here, δ_{opt} refers to the targeted mean shift that requires rapid detection. The optimisation procedure for this ARL-based VSS $\bar{X}$ chart is described in Castagliola et al. (2012). It must be noted that using these optimal charting parameters, the ARLs, SDRLs, and other percentiles of the run-length distribution are evaluated for numerous $\delta \in \{0.0, 0.2, 0.4, 0.6, 0.8, 1.0, 1.5, 2.0, 3.0\}$ in Table 1.

As shown in Table 1, a notable discrepancy between ARL and MRL is observed, especially for $\delta \leq 1.0$. Obviously, in the in-control scenario ($\delta = 0$), the in-control MRL (MRL_0) obtained from all the cases are different though the same $ARL_0 = 370$ is attained. From Table 1, for $n = 3$, the same $ARL_0 = 370$ is obtained for cases with estimated ($m \in \{10, 20, 40, 80\}$) and known ($m = +\infty$) process parameters, however, $MRL_0 \in \{69, 124, 176, 211, 257\}$ for $m \in \{10, 20, 40, 80, +\infty\}$. Though the ARL_0 is the same, it is clear that when m decreases, the values of MRL_0 decrease, indicating an increase in false alarms. This single example demonstrates that the ARL fails to account for the rising occurrence of false alarms in cases involving estimated process parameters, highlighting that the ARL alone may not fully capture the effects of parameter estimations on the chart's overall performance.

Besides, the usage of ARL as the performance measure gives rise to interpretation problems. When $ARL_0 = 370$, there is a risk that practitioners could misinterpret this ARL_0 as a false alarm signal happening at the 370th sample, which is observed in half of the cases. As a matter of fact, this actual value is positioned at the 63rd percentile (Table 1) for the known ($m = +\infty$) process parameters and it keeps on increasing when m decreases. Only the MRL measurement can provide us with stable information regarding the 50% of the time. For example, when $\delta = 0$ and $n = 5$, the false signal happens considerably sooner at the 116th, 172nd, 210th, 232nd, or 257th sample, instead of the 370th ($ARL_0 = 370$) sample, for $m \in \{10, 20, 40, 80, +\infty\}$, in half of the time (Table 1). From this point of view, we observe that the present issue with interpretation for the scenario of known process parameters emerges more serious when dealing with those of estimated process parameters, especially with smaller values of Phase-I samples m. Consequently, misinterpretation issues in a control chart can lead to incorrect decision-making and false conclusions about the process state.

With the implementation of the ARL optimisation procedure for the VSS $\bar{X}$ chart in both scenarios of known and estimated process parameters, Table 1 shows that the lower percentiles, i.e., $\ell_{0.05}$ and $\ell_{0.25}$ of the run-length distribution for the scenarios of estimated process parameters, are shorter than the scenarios of known process parameters. At $\delta = 0$, this phenomenon signifies a greater occurrence of false alarms in the scenario involving estimated process parameters. When $n = 3$ and $\delta = 0$, an early false signal is likely to occur before $\ell_{0.25} \in \{21, 42, 65, 83\}^{th}$ sample for $m \in \{10, 20, 40, 80\}$, respectively, with a probability of 0.25. In contrast, for $m = +\infty$, the early false signal occurs at the 107th sample (Table 1). In the SPC context, excessive false signals are unfavourable by practitioners. Enormous time and cost may be wasted in order to discover non-existent assignable causes, leading to expensive failures in the SPC monitoring scheme.

Given that the middle half of the distribution is bounded by the quartiles, namely $\ell_{0.25}$ and $\ell_{0.75}$, they provide valuable insights into the spread, behaviour, skewness, and variation of the run-length distribution. Similar insights are gained from the extreme percentiles, that are $\ell_{0.05}$ and $\ell_{0.95}$. Table 1 highlights a substantial disparity between

TABLE 1. Exact ARLs, SDRLs, percentile values (5th, 25th, 50th, 75th and 95th percentiles) and the percentages of all the RL $\leq$ ARL$_0$ for the optimal VSS $\bar{X}$ chart with estimated ($m \in \{10, 20, 40, 80\}$) and known ($m = +\infty$) process parameters when $n_1 = n_S$

		$n = 3$					$n = 5$				
		$m = 10$	$m = 20$	$m = 40$	$m = 80$	$m = +\infty$	$m = 10$	$m = 20$	$m = 40$	$m = 80$	$m = +\infty$
	n_S	2	2	2	2	2	3	4	4	4	4
	n_L	13	12	13	13	13	15	15	15	15	15
	W	1.7130	1.6821	1.704	1.6907	1.6754	1.4430	1.7249	1.7017	1.6883	1.6753
δ	K	2.7564	2.8742	2.9402	2.9712	2.9997	2.9052	2.9624	2.9852	2.9938	3.0000
0.0	ARL$_0$	370.00	370.00	370.00	370.00	370.00	370.00	370.00	370.00	370.00	370.00
	SDRL$_0$	3740.64	1122.26	649.15	439.50	369.53	1212.44	666.33	498.91	429.92	369.5
	$\ell_{0.05}$	4	7	11	15	19	6	11	15	17	19
	$\ell_{0.25}$	21	42	65	83	107	39	63	82	94	107
	MRL$_0$	69	124	176	211	257	116	172	210	232	257
	$\ell_{0.75}$	226	339	421	466	513	327	417	465	489	513
	$\ell_{0.95}$	1337	1397	1335	1246	1108	1405	1345	1253	1186	1109
	% of RL$\leq$ARL$_0$	83	77	72	68	63	78	72	68	66	63
0.2	ARL$_1$	306.40	262.49	243.09	230.52	215.01	241.69	215.13	194.24	181.31	166.69
	SDRL$_1$	3034.70	842.86	451.63	321.57	214.32	882.45	429.47	285.99	223.77	166.01
	$\ell_{0.05}$	3	5	7	9	12	4	6	7	8	9
	$\ell_{0.25}$	15	27	40	49	62	20	31	39	43	48
	MRL$_1$	49	82	109	127	149	65	89	102	109	116
	$\ell_{0.75}$	166	232	270	285	298	199	231	236	234	231
	$\ell_{0.95}$	1029	1001	895	792	643	935	810	682	597	498
0.4	ARL$_1$	143.98	102.85	80.96	70.22	59.62	75.54	57.61	46.53	41.27	36.35
	SDRL$_1$	1656.66	370.49	163.69	102.29	58.42	347.33	129.25	71.70	51.18	35.22
	$\ell_{0.05}$	2	3	3	4	4	2	2	3	3	3
	$\ell_{0.25}$	7	10	13	15	18	6	9	10	10	11
	MRL$_1$	20	29	34	38	42	17	22	24	25	26
	$\ell_{0.75}$	70	85	86	85	82	53	58	55	53	50
	$\ell_{0.95}$	468	391	300	243	176	286	217	163	135	107
0.6	ARL$_1$	46.29	28.57	20.45	17.48	15.00	16.48	12.96	10.69	9.73	8.89
	SDRL$_1$	629.53	104.03	37.19	22.05	13.33	79.15	24.84	13.28	9.83	7.41
	$\ell_{0.05}$	2	2	2	2	2	2	2	2	2	2
	$\ell_{0.25}$	4	4	5	5	6	3	3	3	4	4
	MRL$_1$	8	10	10	11	11	6	6	7	7	7
	$\ell_{0.75}$	22	24	22	21	20	13	14	13	12	12
	$\ell_{0.95}$	140	101	69	55	42	54	43	33	28	24

continue to next page

continue from previous page

0.8	ARL_1	13.08	8.74	7.02	6.48	6.04	5.00	4.52	4.16	4.01	3.87
	$SDRL_1$	172.09	21.27	7.92	5.63	4.32	12.21	4.78	3.23	2.77	2.41
	$\ell_{0.05}$	1	1	2	2	2	1	1	1	1	1
	$\ell_{0.25}$	2	3	3	3	3	2	2	2	2	2
	MRL_1	4	5	5	5	5	3	3	3	3	3
	$\ell_{0.75}$	9	9	8	8	8	5	5	5	5	5
	$\ell_{0.95}$	36	26	19	17	15	13	12	10	9	9
1.0	ARL_1	5.05	4.28	3.98	3.87	3.76	2.83	2.67	2.60	2.57	2.53
	$SDRL_1$	34.89	4.65	2.88	2.51	2.24	2.25	1.65	1.41	1.32	1.24
	$\ell_{0.05}$	1	1	1	1	1	1	1	1	1	1
	$\ell_{0.25}$	2	2	2	2	2	2	2	2	2	2
	MRL_1	3	3	3	3	3	2	2	2	2	2
	$\ell_{0.75}$	5	5	5	5	5	3	3	3	3	3
	$\ell_{0.95}$	13	11	9	9	8	6	6	5	5	5
1.5	ARL_1	2.20	2.19	2.22	2.21	2.21	1.72	1.55	1.55	1.55	1.55
	$SDRL_1$	1.34	1.12	1.06	1.01	0.97	0.69	0.64	0.62	0.61	0.60
	$\ell_{0.05}$	1	1	1	1	1	1	1	1	1	1
	$\ell_{0.25}$	1	2	2	2	2	1	1	1	1	1
	MRL_1	2	2	2	2	2	2	1	1	1	1
	$\ell_{0.75}$	3	3	3	3	3	2	2	2	2	2
	$\ell_{0.95}$	5	4	4	4	4	3	3	3	3	2
2.0	ARL_1	1.57	1.60	1.63	1.64	1.65	1.31	1.16	1.16	1.16	1.16
	$SDRL_1$	0.72	0.68	0.67	0.66	0.64	0.48	0.38	0.37	0.37	0.37
	$\ell_{0.05}$	1	1	1	1	1	1	1	1	1	1
	$\ell_{0.25}$	1	1	1	1	1	1	1	1	1	1
	MRL_1	1	2	2	2	2	1	1	1	1	1
	$\ell_{0.75}$	2	2	2	2	2	2	1	1	1	1
	$\ell_{0.95}$	3	3	3	3	3	2	2	2	2	2
3.0	ARL_1	1.09	1.10	1.1	1.11	1.11	1.02	1.00	1.00	1.00	1.00
	$SDRL_1$	0.29	0.30	0.31	0.31	0.312	0.13	0.04	0.04	0.04	0.04
	$\ell_{0.05}$	1	1	1	1	1	1	1	1	1	1
	$\ell_{0.25}$	1	1	1	1	1	1	1	1	1	1
	MRL_1	1	1	1	1	1	1	1	1	1	1
	$\ell_{0.75}$	1	1	1	1	1	1	1	1	1	1
	$\ell_{0.95}$	2	2	2	2	2	1	1	1	1	1

$\ell_{0.05}$ and $\ell_{0.95}$, especially in situations where the process remains in-control or shows only marginal deviations from in-control (referred to as the out-of-control situation). As δ decreases, the difference becomes more pronounced. For instance, when $n = 3$, $m = 10$, and $\delta \in \{0.0, 0.2, 0.4, 0.6\}$, the disparity between $\ell_{0.05}$ and $\ell_{0.95}$ is {1333, 1026, 466, 138}, respectively. When n increases from 3 to 5, the run-length distribution of the VSS $\bar{X}$ chart exhibits similar trends under the scenarios of estimated process parameters.

Additionally, Figure 2 shows the plots of pmf $f_{\mathrm{RL}}(\ell)$ for the RL of the VSS $\bar{X}$ chart, considering $m \in \{10, 20, 40, 80, +\infty\}$, $\mathrm{ARL}_0 = 370$, $\mathrm{ASS}_0 = n = 3$, and $\delta \in \{0.0, 0.5, 1.0, 2.0\}$. The plots show that as the value of δ increases, the skewness of the run-length distribution reduces. Specifically, when $\delta = 0$, the highest skewness is observed for the run-length distribution of the VSS $\bar{X}$ chart based on estimated process parameters, while the run-length distribution approaches symmetry when $\delta = 2.0$. Differences in skewness at various shifts will lead to interpretation challenges for practitioners. Therefore, it is crucial to introduce more robust measures, such as MRL and EMRL, to assess the performance of the run-length distribution for the proposed VSS $\bar{X}$ chart using estimated process parameters. The following sections outline the development of optimal statistical designs using the MRL and EMRL metrics to attain the most effective detection speed for both specific and overall shift sizes, respectively.

MRL-BASED OPTIMISATION OF THE VSS $\bar{X}$ CHART USING ESTIMATED PROCESS PARAMETERS

In real-world settings, practitioners seek to identify the optimal or best charting parameters for a control chart to achieve the most accurate and timely detection of process deviations. First, we propose an optimal statistical design for the VSS $\bar{X}$ chart using estimated process parameters, which focuses on the minimisation of the $\mathrm{MRL}_1(\delta_{\mathrm{opt}})$ for known shift-size cases. Here, $\mathrm{MRL}_1(\delta_{\mathrm{opt}})$ refers to the out-of-control MRL (MRL_1) corresponding to a designated process shift size δ_{opt}, aimed at achieving quicker detection speeds. Mathematically, the optimal statistical design is shown as follows:

$$\mathrm{Minimise}_{(n_S, n_L, W, K)} \mathrm{MRL}_1(\delta_{\mathrm{opt}}), \tag{15}$$

subject to the constraints

$$\mathrm{MRL}_0 = \tau, \tag{16}$$

$$\mathrm{ASS}_0 = n, \text{ and} \tag{17}$$

$$1 \leq n_S < n < n_L \leq n_{\max}, \tag{18}$$

where τ and n represent the prespecified values for the in-control MRL and ASS, respectively. In Equation (18), $n_{\max}$ is the maximum sample size, set to 15. This sample

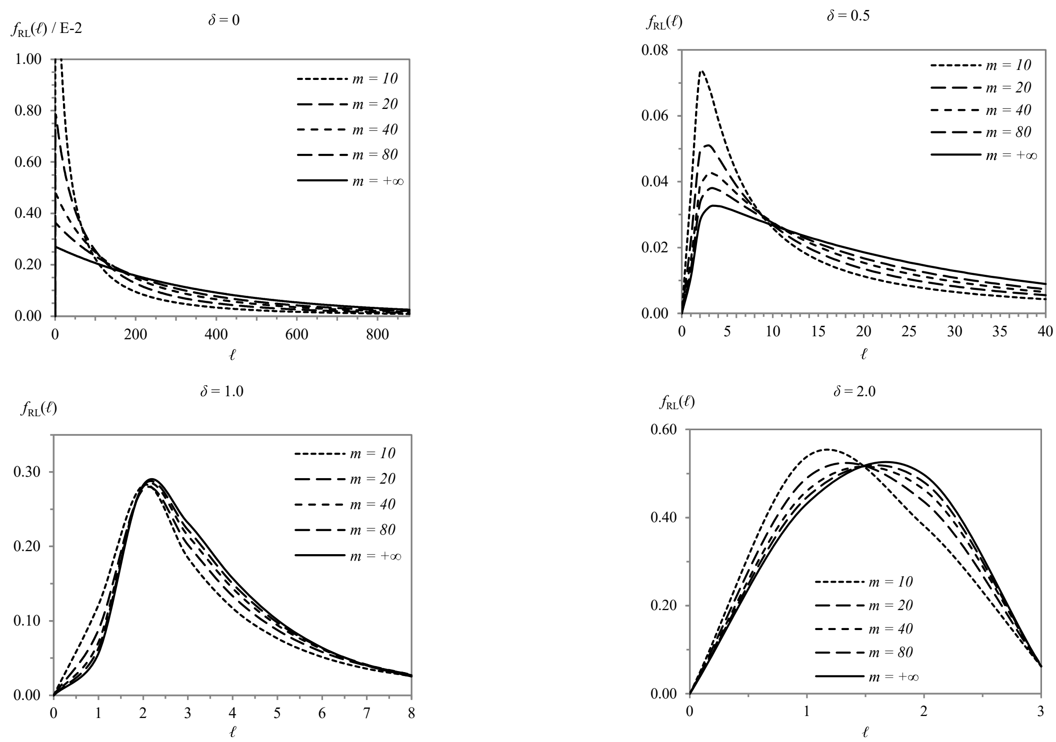

FIGURE 2. The pmf $f_{\mathrm{RL}}(\ell)$ plots of the VSS $\bar{X}$ chart's run length when $m \in \{10, 20, 40, 80, +\infty\}$, $\mathrm{ARL}_0 = 370$, $\mathrm{ASS}_0 = n = 3$ and $\delta \in \{0, 0.5, 1.0, 2.0\}$

size is sufficiently large to identify meaningful process mean shifts, while minimising the time and resources required for data collection and analysis in an industrial setting. The value of $n_{\max} = 15$ is also employed by Castagliola et al. (2012) and Hu et al. (2016) in their studies. However, in industry applications, researchers and practitioners may customise the value of $n_{\max}$ based on the operational needs and performance objectives of their specific processes. The steps herewith detail the process for determining the optimal charting parameters (n_S, n_L, W, K) for the VSS $\bar{X}$ chart using estimated process parameters:

Step 1 Specify the targeted values for τ, n, m, $n_{\max}$, and δ_{opt}.

Step 2 Choose a pair of (n_S, n_L) that satisfies constraint (18).

Step 3 Utilise a nonlinear equation solver to search the (W, K) values that fulfil constraints (16) and (17), when $\delta = 0$.

Step 4 Using the predetermined charting parameters (n_S, n_L, W, K) from Steps 2 and 3, evaluate the objective function $\text{MRL}_1(\delta_{\text{opt}})$ using Equations (8) and (9), with $\epsilon = 0.5$.

Step 5 Perform Steps 2 to 4 repeatedly to find all the possible combinations of (n_S, n_L, W, K) for the VSS $\bar{X}$ chart using estimated process parameters when $\delta = 0$, which satisfy constraints (16) - (18).

Step 6 Determine the optimal (n_S, n_L, W, K) combination for the VSS $\bar{X}$ chart using estimated process parameters that yields the most minimum MRL_1 value for any out-of-control case $(\delta \neq 0)$.

By applying the MRL optimisation model (15) - (18), the corresponding optimal charting parameters (n_S, n_L, W, K) for the VSS $\bar{X}$ chart using estimated process parameters can be determined. Tables 2 and 3 present the optimal (n_S, n_L, W, K) parameters for the VSS $\bar{X}$ chart, and the corresponding $(\ell_{0.05}, \text{MRL}, \ell_{0.95})$ values, when $m \in \{10, 20, 40, 80, +\infty\}$, $\text{MRL}_0 = \tau = 250$, $\text{ASS}_0 = n \in \{3, 5, 7, 9\}$ and $\delta_{\text{opt}} \in \{0.2, 0.4, 0.6, 0.8, 1.0, 1.5, 2.0\}$ for $n_1 = n_S$ and $n_1 = n_L$, respectively. As a numeric example, from Table 2, for $n = 3$, and $\delta_{\text{opt}} = 0.4$, the VSS $\bar{X}$ chart with $m = 20$ is optimised for the charting parameters $(n_S, n_L, W, K) = (1, 15, 1.5130, 3.1100)$ and its corresponding $(\ell_{0.05}, \text{MRL}_1, \ell_{0.95}) = (3, 36, 730)$. This also means that the chart is capable of signalling a process mean shift by the 3rd, 36th, and 730th samples, respectively, in 5%, 50%, and 95% of the time.

Regardless of whether $n_1 = n_S$ or $n_1 = n_L$, for any fixed n and $\delta_{\text{opt}} \leq 1.0$, the detection performances of the VSS $\bar{X}$ charts with various values of m significantly differ from that those with the scenarios of known $(m = +\infty)$ process parameters (Tables 2 & 3). For $\delta_{\text{opt}} \geq 1.50$, all the VSS $\bar{X}$ charts, whether based on known or estimated process parameters exhibit similar $(\ell_{0.05}, \text{MRL}_1, \ell_{0.95})$ performances. As an example, when $n = 5$, $\delta_{\text{opt}} = 1.5$, and $n_1 = n_L$, the $(\ell_{0.05}, \text{MRL}_1, \ell_{0.95})$ values for the VSS $\bar{X}$ charts are {(1, 1, 1), (1, 1, 1), (1, 1, 1), (1, 1, 1), (1, 1, 1)} for $m \in \{10, 20, 40, 80, +\infty\}$, respectively (Table 3). Remarkably, when m becomes larger, particularly at $m = 80$, the run-length performance of the VSS $\bar{X}$ chart using estimated process parameters closely approaches that of the scenario with known $(m = +\infty)$ process parameters. Therefore, to obtain comparable MRL_1 performance with that of the scenario with known process parameters, practitioners are recommended to choose $m \geq 80$. Nonetheless, it is noteworthy that selecting a large sample size m in the Phase-I process increases sampling costs, which may be economically unfavourable.

EMRL-BASED OPTIMISATION OF THE VSS $\bar{X}$ CHART USING ESTIMATED PROCESS PARAMETERS

In real-world scenarios, having complete knowledge of the exact and actual shift size beforehand is rarely feasible. In cases where the actual shift size of a process is uncertain and deviates from δ_{opt}, it can result in unsatisfactory performance for the control charts designed using the MRL optimisation model (15) - (18) for a specific shift size. In such instances, the control chart may fail to promptly detect smaller or larger process shifts than anticipated, leading to increased false alarms or delayed detection. Therefore, to enhance effective signalling performance over a process shift-size domain, the EMRL optimisation is implemented for the proposed VSS $\bar{X}$ chart using estimated process parameters. The mathematical formulation for the EMRL optimisation model under the cases with unknown shift sizes is detailed below:

$$\text{Minimise}_{(n_S, n_L, W, K)} \text{EMRL}, \tag{19}$$

subject to the same constraints (16) - (18) in the MRL optimisation model discussed in the previous section. The computation of EMRL is

$$\text{EMRL} = \int_{\delta_{\min}}^{\delta_{\max}} f_\delta(\delta) \text{MRL}\, d\delta, \tag{20}$$

where $f_\delta(\delta)$ represents the pdf of δ. Here, the process mean shift size is modelled as a uniform distribution $U(\delta_{\min}, \delta_{\max})$, where $\delta_{\min}$ and $\delta_{\max}$ represent the minimum and maximum shift values, respectively. Throughout this paper, we use the shift-size domain $(\delta_{\min}, \delta_{\max}] = (0, 2]$.

The process of identifying the optimal (n_S, n_L, W, K) parameters for the VSS $\bar{X}$ chart, by using the developed EMRL optimisation model is performed through the following steps:

TABLE 2. The optimal charting parameters (n_S, n_L, W, K) (first row of each cell) and the ($\ell_{0.05}$, MRL$_1$, $\ell_{0.95}$) values (second row of each cell) of the VSS $\bar{X}$ chart when $m \in \{10, 20, 40, 80, +\infty\}$, MRL$_0$ = 250, ASS$_0$ = $n \in \{3, 5, 7, 9\}$, $n_1 = n_S$ and $\delta_{\text{opt}} \in \{0.2, 0.4, 0.6, 0.8, 1.0, 1.5, 2.0\}$

δ_{opt}	$m = 10$ (n_S, n_L, W, K) ($\ell_{0.05}$, MRL$_1$, $\ell_{0.95}$)	$m = 20$ (n_S, n_L, W, K) ($\ell_{0.05}$, MRL$_1$, $\ell_{0.95}$)	$m = 40$ (n_S, n_L, W, K) ($\ell_{0.05}$, MRL$_1$, $\ell_{0.95}$)	$m = 80$ (n_S, n_L, W, K) ($\ell_{0.05}$, MRL$_1$, $\ell_{0.95}$)	$m = +\infty$ (n_S, n_L, W, K) ($\ell_{0.05}$, MRL$_1$, $\ell_{0.95}$)
			$n = 3$		
0.2	(1, 15, 1.5690, 3.2098) (5, 153, 7429)	(1, 15, 1.5130, 3.1100) (7, 145, 2473)	(1, 15, 1.4835, 3.0547) (9, 141, 1312)	(1, 15, 1.4686, 3.0246) (10, 139, 915)	(1, 15, 1.4537, 2.9922) (11, 139, 597)
0.4	(1, 15, 1.5690, 3.2098) (3, 42, 2610)	(1, 15, 1.5130, 3.1100) (3, 36, 730)	(1, 15, 1.4835, 3.0547) (3, 34, 345)	(1, 15, 1.4686, 3.0246) (4, 33, 222)	(1, 15, 1.4537, 2.9922) (4, 32, 133)
0.6	(1, 15, 1.5690, 3.2098) (2, 11, 442)	(1, 15, 1.5130, 3.1100) (2, 10, 120)	(1, 15, 1.4835, 3.0547) (2, 9, 60)	(1, 15, 1.4686, 3.0246) (2, 9, 43)	(1, 15, 1.4537, 2.9922) (2, 9, 31)
0.8	(1, 15, 1.5690, 3.2098) (2, 6, 60)	(1, 15, 1.5130, 3.1100) (2, 5, 25)	(1, 15, 1.4835, 3.0547) (2, 5, 18)	(1, 15, 1.4686, 3.0246) (2, 5, 15)	(1, 15, 1.4537, 2.9922) (2, 5, 13)
1.0	(1, 14, 1.5252, 3.2082) (2, 4, 17)	(2, 12, 1.7018, 3.1044) (1, 3, 12)	(2, 10, 1.5535, 3.0524) (1, 3, 10)	(1, 12, 1.3381, 3.0243) (2, 3, 9)	(2, 10, 1.5216, 2.9922) (1, 3, 8)
1.5	(2, 7, 1.3652, 3.1905) (1, 2, 5)	(2, 7, 1.3197, 3.1024) (1, 2, 4)	(2, 6, 1.1623, 3.0518) (1, 2, 4)	(1, 7, 0.9680, 3.0239) (1, 2, 4)	(1, 6, 0.8347, 2.9922) (1, 2, 4)
2.0	(1, 6, 0.8833, 3.1933) (1, 2, 3)	(1, 5, 0.6866, 3.1023) (1, 2, 3)	(2, 7, 1.2961, 3.0520) (1, 2, 2)	(2, 6, 1.1522, 3.0237) (1, 2, 2)	(2, 6, 1.1420, 2.9922) (1, 2, 2)
			$n = 5$		
0.2	(1, 15, 1.1204, 3.1678) (6, 123, 2522)	(1, 15, 1.0910, 3.0877) (7, 113, 1212)	(1, 15, 1.0755, 3.0424) (8, 108, 782)	(1, 15, 1.0676, 3.0179) (8, 106, 605)	(1, 15, 1.0597, 2.9922) (9, 104, 447)
0.4	(1, 15, 1.1204, 3.1678) (3, 25, 598)	(1, 15, 1.0910, 3.0877) (3, 22, 242)	(1, 15, 1.0755, 3.0424) (3, 21, 143)	(1, 15, 1.0676, 3.0179) (3, 20, 107)	(1, 15, 1.0597, 2.9922) (3, 19, 78)
0.6	(1, 15, 1.1204, 3.1678) (2, 7, 81)	(2, 15, 1.2262, 3.0864) (2, 6, 40)	(1, 15, 1.0755, 3.0424) (2, 6, 26)	(1, 15, 1.0676, 3.0179) (2, 6, 22)	(1, 15, 1.0597, 2.9922) (2, 6, 18)
0.8	(1, 15, 1.1204, 3.1678) (2, 4, 17)	(3, 15, 1.4169, 3.0849) (1, 3, 11)	(2, 15, 1.2080, 3.0419) (2, 3, 9)	(2, 14, 1.1507, 3.0177) (2, 3, 9)	(2, 14, 1.1420, 2.9922) (2, 3, 8)
1.0	(3, 14, 1.4090, 3.1599) (1, 2, 7)	(3, 12, 1.2492, 3.0839) (1, 2, 6)	(3, 13, 1.2922, 3.0411) (1, 2, 5)	(2, 15, 1.1989, 3.0177) (1, 2, 5)	(2, 14, 1.1420, 2.9922) (1, 2, 5)
1.5	(2, 9, 0.8268, 3.1572) (1, 2, 3)	(2, 8, 0.6857, 3.0828) (1, 2, 3)	(4, 12, 1.5462, 3.0407) (1, 2, 2)	(4, 10, 1.3836, 3.0173) (1, 2, 2)	(4, 10, 1.3725, 2.9922) (1, 1, 2)
2.0	(3, 6, 0.4439, 3.1521) (1, 1, 2)	(3, 6, 0.4346, 3.0814) (1, 1, 2)	(3, 6, 0.4296, 3.0402) (1, 1, 2)	(3, 6, 0.4271, 3.0172) (1, 1, 2)	(3, 6, 0.4244, 2.9922) (1, 1, 2)

continue to next page

continue from previous page

			$n = 7$		
0.2	(1, 15, 0.8251, 3.1491) (6, 104, 1555)	(1, 15, 0.8056, 3.0780) (6, 94, 847)	(1, 15, 0.7954, 3.0374) (7, 89, 581)	(1, 15, 0.7902, 3.0154) (7, 87, 466)	(1, 15, 0.7849, 2.9922) (7, 85, 361)
0.4	(1, 15, 0.8251, 3.1491) (3, 19, 284)	(1, 15, 0.8056, 3.0780) (3, 17, 137)	(1, 15, 0.7954, 3.0374) (3, 16, 91)	(1, 15, 0.7902, 3.0154) (3, 15, 74)	(1, 15, 0.7849, 2.9922) (3, 15, 59)
0.6	(1, 15, 0.8251, 3.1491) (2, 6, 40)	(1, 15, 0.8056, 3.0780) (2, 5, 24)	(1, 15, 0.7954, 3.0374) (2, 5, 19)	(1, 15, 0.7902, 3.0154) (2, 5, 17)	(1, 15, 0.7849, 2.9922) (2, 5, 15)
0.8	(1, 15, 0.8251, 3.1491) (2, 3, 11)	(2, 15, 0.8857, 3.0775) (2, 3, 8)	(2, 15, 0.8742, 3.0372) (2, 3, 7)	(1, 15, 0.7902, 3.0154) (2, 3, 7)	(3, 15, 0.9601, 2.9922) (1, 3, 6)
1.0	(2, 15, 0.9078, 3.1478) (1, 2, 5)	(3, 15, 0.9865, 3.0769) (1, 2, 4)	(3, 14, 0.9137, 3.0369) (1, 2, 4)	(2, 15, 0.8683, 3.0153) (1, 2, 4)	(2, 13, 0.7412, 2.9922) (1, 2, 4)
1.5	(5, 10, 0.8786, 3.1403) (1, 1, 2)	(5, 9, 0.6853, 3.0742) (1, 1, 2)	(5, 8, 0.4296, 3.0359) (1, 1, 2)	(5, 8, 0.4270, 3.0149) (1, 1, 2)	(4, 9, 0.5180, 2.9922) (1, 1, 2)
2.0	(3, 8, 0.2570, 3.1393) (1, 1, 2)	(6, 8, 0.6854, 3.0738) (1, 1, 1)	(6, 8, 0.6769, 3.0359) (1, 1, 1)	(6, 8, 0.6724, 3.0149) (1, 1, 1)	(6, 8, 0.6679, 2.9922) (1, 1, 1)
			$n = 9$		
0.2	(1, 15, 0.5866, 3.1382) (5, 90, 1143)	(1, 15, 0.5736, 3.0725) (6, 81, 659)	(1, 15, 0.5667, 3.0346) (6, 77, 467)	(1, 15, 0.5631, 3.0140) (6, 74, 383)	(1, 15, 0.5596, 2.9922) (6, 72, 307)
0.4	(1, 15, 0.5866, 3.1382) (2, 16, 177)	(1, 15, 0.5736, 3.0725) (2, 14, 97)	(1, 15, 0.5667, 3.0346) (2, 14, 70)	(1, 15, 0.5631, 3.0140) (2, 13, 59)	(1, 15, 0.5596, 2.9922) (2, 13, 50)
0.6	(1, 15, 0.5866, 3.1382) (2, 5, 29)	(7, 15, 1.1734, 3.0708) (1, 4, 21)	(4, 15, 0.7509, 3.0344) (2, 4, 16)	(3, 15, 0.6723, 3.0140) (2, 4, 14)	(2, 15, 0.6087, 2.9922) (2, 4, 13)
0.8	(7, 15, 1.2041, 3.1339) (1, 2, 9)	(6, 15, 0.9858, 3.0712) (1, 2, 7)	(5, 15, 0.8485, 3.0343) (1, 2, 6)	(5, 15, 0.8403, 3.0319) (1, 2, 6)	(7, 15, 1.1420, 2.9922) (1, 2, 5)
1.0	(3, 15, 0.7013, 3.1369) (1, 2, 4)	(2, 14, 0.5557, 3.0718) (1, 2, 4)	(6, 15, 0.9730, 3.0342) (1, 2, 3)	(5, 15, 0.8403, 3.0139) (1, 2, 3)	(4, 15, 0.7412, 2.9922) (1, 2, 3)
1.5	(5, 10, 0.2574, 3.1320) (1, 1, 2)	(5, 10, 0.2524, 3.0700) (1, 1, 2)	(5, 10, 0.2498, 3.0338) (1, 1, 2)	(5, 10, 0.2484, 3.0138) (1, 1, 2)	(4, 10, 0.2039, 2.9922) (1, 1, 2)
2.0	(6, 10, 0.3262, 3,1319) (1, 1, 1)	(6, 10, 0.3195, 3.0699) (1, 1, 1)	(6, 10, 0.3160, 3.0338) (1, 1, 1)	(6, 10, 0.3141, 3.0138) (1, 1, 1)	(6, 10, 0.3123, 2.9922) (1, 1, 1)

TABLE 3. The optimal charting parameters (n_S, n_L, W, K) (first row of each cell) and the ($\ell_{0.05}$, MRL_1, $\ell_{0.95}$) values (second row of each cell) of the VSS $\bar{X}$ chart when $m \in \{10, 20, 40, 80, +\infty\}$, $MRL_0 = 250$, $ASS_0 = n \in \{3, 5, 7, 9\}$, $n_1 = n_L$ and $\delta_{opt} \in \{0.2, 0.4, 0.6, 0.8, 1.0, 1.5, 2.0\}$

δ_{opt}	$m = 10$ (n_S, n_L, W, K) ($\ell_{0.05}$, MRL_1, $\ell_{0.95}$)	$m = 20$ (n_S, n_L, W, K) ($\ell_{0.05}$, MRL_1, $\ell_{0.95}$)	$m = 40$ (n_S, n_L, W, K) ($\ell_{0.05}$, MRL_1, $\ell_{0.95}$)	$m = 80$ (n_S, n_L, W, K) ($\ell_{0.05}$, MRL_1, $\ell_{0.95}$)	$m = +\infty$ (n_S, n_L, W, K) ($\ell_{0.05}$, MRL_1, $\ell_{0.95}$)
			$n = 3$		
0.2	(1, 15, 1.6357, 3.2029) (2, 155,7466)	(1, 15, 1.5490, 3.1084) (4, 146, 2499)	(1, 15, 1.5099, 3.0542) (6, 141, 1325)	(1, 15, 1.4916, 3.0244) (7, 139, 924)	(1, 15, 1.4740, 2.9922) (9, 138, 603)
0.4	(1, 15, 1.6357, 3.2029) (1, 40, 2733)	(1, 15, 1.5490, 3.1084) (1, 33, 755)	(1, 15, 1.5099, 3.0542) (1, 30, 352)	(1, 15, 1.4916, 3.0244) (1, 29, 225)	(1, 15, 1.4740, 2.9922) (1, 28, 132)
0.6	(1, 15, 1.6357, 3.2029) (1, 6, 484)	(1, 15, 1.5490, 3.1084) (1, 5, 121)	(1, 15, 1.5099, 3.0542) (1, 4, 57)	(1, 15, 1.4916, 3.0244) (1, 4, 38)	(1, 15, 1.4740, 2.9922) (1, 4, 26)
0.8	(1, 15, 1.6357, 3.2029) (1, 2, 60)	(1, 15, 1.5490, 3.1084) (1, 1, 19)	(1, 15, 1.5099, 3.0542) (1, 1, 11)	(1, 15, 1.4916, 3.0244) (1, 1, 8)	(1, 15, 1.4740, 2.9922) (1, 1, 6)
1.0	(1, 15, 1.6357, 3.2029) (1, 1, 8)	(1, 14, 1.5055, 3.1079) (1, 1, 4)	(1, 14, 1.4685, 3.0540) (1, 1, 3)	(1, 13, 1.4065, 3.0243) (1, 1, 3)	(2, 15, 1.7844, 2.9922) (1, 1, 2)
1.5	(2, 13, 1.9137, 3.1909) (1, 1, 1)	(2, 11, 1.6901, 3.1030) (1, 1, 1)	(2, 11, 1.6457, 3.0522) (1, 1, 1)	(2, 10, 1.5630, 3.0238) (1, 1, 1)	(2, 10, 1.5440, 2.9922) (1, 1, 1)
2.0	(2, 7, 1.4088, 3.1887) (1, 1, 1)	(2, 7, 1.3460, 3.1019) (1, 1, 1)	(2, 6, 1.1796, 3.0517) (1, 1, 1)	(2, 6, 1.1674, 3.0236) (1, 1, 1)	(2, 6, 1.1554, 2.9922) (1, 1, 1)
			$n = 5$		
0.2	(1, 15, 1.1450, 3.1660) (3, 123, 2537)	(1, 15, 1.1076, 3.0871) (5, 113,1220)	(1, 15, 1.0895, 3.0422) (6, 107, 787)	(1, 15, 1.0807, 3.0178) (6, 105, 609)	(1, 15, 1.0720, 2.9922) (7, 104, 450)
0.4	(1, 15, 1.1450, 3.1660) (1, 22, 608)	(1, 15, 1.1076, 3.0871) (1, 19, 244)	(1, 15, 1.0895, 3.0422) (1, 18, 142)	(1, 15, 1.0807, 3.0178) (1, 17, 105)	(1, 15, 1.0720, 2.9922) (1, 17, 76)
0.6	(1, 15, 1.1450, 3.1660) (1, 4, 80)	(1, 15, 1.1076, 3.0871) (1, 4, 35)	(1, 15, 1.0895, 3.0422) (1, 3, 23)	(1, 15, 1.0807, 3.0178) (1, 3, 19)	(1, 15, 1.0720, 2.9922) (1, 3, 15)
0.8	(1, 15, 1.1450, 3.1660) (1, 2, 13)	(2, 15, 1.2455, 3.0858) (1, 1, 8)	(2, 15, 1.2243, 3.0417) (1, 1, 6)	(1, 15, 1.0807, 3.0178) (1, 1, 5)	(2, 14, 1.1554, 2.9922) (1, 1, 5)
1.0	(2, 14, 1.2363, 3.1618) (1, 1, 4)	(3, 14, 1.3904, 3.0841) (1, 1, 3)	(4, 13, 1.6349, 3.0405) (1, 1, 3)	(3, 15, 1.4029, 3.0175) (1, 1, 2)	(4, 15, 1.7039, 2.9922) (1, 1, 2)
1.5	(4, 12, 1.6653, 3.1539) (1, 1,1)	(4, 11, 1.5286, 3.0821) (1, 1, 1)	(4, 11, 1.5009, 3.0404) (1, 1, 1)	(4, 10, 1.4028, 3.0173) (1, 1, 1)	(4, 10, 1.3906, 2.9922) (1, 1, 1)

continue to next page

continue from previous page

2.0	(4, 7, 1.0339, 3.1521) (1, 1, 1)	(4, 6, 0.6971, 3.0812) (1, 1, 1)	(4, 6, 0.6869, 3.0401) (1, 1, 1)	(4, 6, 0.6818, 3.0172) (1, 1, 1)	(4, 6, 0.6766, 2.9922) (1, 1, 1)
$n = 7$					
0.2	(1, 15, 0.8407, 3.1483) (4, 103,1561)	(1, 15, 0.8174, 3.0777) (5, 93, 850)	(1, 15, 0.8058, 3.0373) (5, 88, 583)	(1, 15, 0.8001, 3.0153) (6, 86, 468)	(1, 15, 0.7944, 2.9922) (6, 84, 363)
0.4	(1, 15, 0.8407, 3.1483) (1, 17, 285)	(1, 15, 0.8174, 3.0777) (1, 15, 136)	(1, 15, 0.8058, 3.0373) (1, 14, 90)	(1, 15, 0.8001, 3.0153) (1, 14, 72)	(1, 15, 0.7944, 2.9922) (1, 13,57)
0.6	(2, 15, 0.9244, 3.1470) (1, 4, 39)	(2, 15, 0.8982, 3.0772) (1, 3, 22)	(3, 15, 0.9855, 3.0369) (1, 3, 17)	(3, 15, 0.9783, 3.0152) (1, 3, 15)	(4, 15, 1.1014, 2.9922) (1, 3, 13)
0.8	(5, 15, 1.3715, 3.1424) (1, 2, 9)	(4, 15, 1.1352, 3.0761) (1, 1, 6)	(4, 15, 1.1181, 3.0367) (1, 1, 5)	(5, 15, 1.2979, 3.0151) (1, 1, 5)	(5, 14, 1.2263, 2.9922) (1, 1, 5)
1.0	(5, 15, 1.3715, 3.1424) (1, 1, 3)	(5, 13, 1.1911, 3.0750) (1, 1, 3)	(4, 12, 0.9034, 3.0364) (1, 1, 3)	(6, 15, 1.6177, 3.0150) (1, 1, 2)	(6, 15, 1.6043, 2.9922) (1,1, 2)
1.5	(6, 11, 1.3700, 3.1395) (1, 1, 1)	(6, 11, 1.3285, 3.0742) (1, 1, 1)	(6, 10, 1.1730, 3.0360) (1, 1, 1)	(6, 10, 1.1642, 3.0149) (1, 1, 1)	(6, 10, 1.1554, 2.9922) (1, 1, 1)
2.0	(6, 8, 0.7150, 3.1385) (1, 1, 1)	(6, 8, 0.6959, 3.0738) (1, 1, 1)	(6, 8, 0.6863, 3.0359) (1, 1, 1)	(6, 8, 0.6815, 3.0149) (1, 1, 1)	(6, 8, 0.6766, 2.9922) (1, 1, 1)
$n = 9$					
0.2	(2, 15, 0.6510, 3.1371) (4, 90,1149)	(1, 15, 0.5832, 3.0723) (5, 81,661)	(1, 15, 0.5754, 3.0345) (5, 76, 469)	(1, 15, 0.5716, 3.0140) (5, 73, 384)	(1, 15, 0.5677, 2.9922) (5, 71, 308)
0.4	(1, 15, 0.5987, 3.1377) (1, 14, 177)	(1, 15, 0.5832, 3.0723) (1, 13, 96)	(1, 15, 0.5754, 3.0345) (1, 12, 69)	(1, 15, 0.5716, 3.0140) (1, 12,58)	(1, 15, 0.5677, 2.9922) (1, 11, 49)
0.6	(3, 15, 0.7142, 3.1365) (1, 4, 27)	(5, 15, 0.8684, 3.0713) (1, 3, 18)	(1, 15, 0.5754, 3.0345) (1, 3, 14)	(5, 15, 0.8505, 3.0139) (1, 3,13)	(6, 15, 0.9711, 2.9922) (1, 3, 12)
0.8	(6, 15, 1.0272, 3.1345) (1, 2, 7)	(8, 15, 1.5196, 3.0703) (1, 1,6)	(8, 15, 1.4966, 3.0339) (1, 1, 5)	(8, 15, 1.4852, 3.0138) (1, 1, 5)	(6, 15, 0.9711, 2.9922) (1, 1, 4)
1.0	(8, 14, 1.4759, 3.1324) (1, 1, 3)	(8, 13, 1.3263, 3.0701) (1, 1, 3)	(7, 15, 1.1723, 3.0340) (1,1,2)	(8, 15, 1.4852, 3.0138) (1, 1, 2)	(8, 15, 1.4740, 2.9922) (1, 1, 2)
1.5	(8, 11, 1.0263, 3.1318) (1, 1, 1)	(8, 11, 0.9987, 3.0699) (1, 1, 1)	(8, 10, 0.6860, 3.0337) (1, 1, 1)	(8, 10, 0.6814, 3.0138) (1, 1, 1)	(8, 10, 0.6766, 2.9922) (1, 1, 1)
2.0	(8, 10, 0.7137, 3.1315) (1, 1, 1)	(8, 10, 0.6953, 3.0698) (1, 1, 1)	(8, 10, 0.6860, 3.0337) (1, 1, 1)	(8, 10, 0.6814, 3.0138) (1, 1, 1)	(8, 10, 0.6766, 2.9922) (1, 1, 1)

TABLE 4. The optimal charting parameters (n_S, n_L, W, K) and the EMRL values of the VSS $\bar{X}$ chart, together with ($\ell_{0.05}$, MRL_1, $\ell_{0.95}$) values corresponding to specific shift sizes $\delta \in \{0.2, 0.4, 0.6, 0.8, 1.0, 1.5, 2.0\}$, when $m \in \{10, 20, 40, 80, +\infty\}$, $\text{MRL}_0 = 250$, $\text{ASS}_0 = n \in \{3, 5, 7, 9\}$ and $n_1 = n_S$

δ	$m = 10$	$m = 20$	$m = 40$	$m = 80$	$m = +\infty$
	(n_S, n_L, W, K) EMRL ($\ell_{0.05}$, MRL_1, $\ell_{0.95}$)	(n_S, n_L, W, K) EMRL ($\ell_{0.05}$, MRL_1, $\ell_{0.95}$)	(n_S, n_L, W, K) EMRL ($\ell_{0.05}$, MRL_1, $\ell_{0.95}$)	(n_S, n_L, W, K) EMRL ($\ell_{0.05}$, MRL_1, $\ell_{0.95}$)	(n_S, n_L, W, K) EMRL ($\ell_{0.05}$, MRL_1, $\ell_{0.95}$)
			$n = 3$		
	(1, 15, 1.5690, 3.2098) 24.46	(1, 15, 1.5130, 3.1100) 22.73	(1, 15, 1.4835, 3.0547) 22.12	(1, 15, 1.4686, 3.0246) 21.76	(1, 15, 1.4537, 2.9922) 21.43
0.2	(5, 153, 7429)	(7, 145, 2473)	(9, 141, 1312)	(10, 139, 915)	(11, 139, 597)
0.4	(3, 42, 2610)	(3, 36, 730)	(3, 34, 345)	(4, 33, 222)	(4, 32, 133)
0.6	(2, 11, 442)	(2, 10, 120)	(2, 9, 60)	(2, 9, 43)	(2, 9, 31)
0.8	(2, 6, 60)	(2, 5, 25)	(2, 5, 18)	(2, 5, 15)	(2, 5, 13)
1.0	(2, 4, 17)	(2, 4, 12)	(2, 4, 10)	(2, 4, 10)	(2, 3, 9)
1.5	(1, 2, 7)	(1, 2, 6)	(1, 2, 6)	(1, 2, 6)	(1, 2, 5)
2.0	(1, 2, 4)	(1, 2, 4)	(1, 2, 4)	(1, 2, 4)	(1, 2, 4)
			$n = 5$		
	(2, 15, 1.2616, 3.1644) 18.89	(1, 15, 1.0910, 3.0877) 17.39	(1, 15, 1.0755, 3.0424) 16.87	(1, 15, 1.0676, 3.0179) 16.48	(1, 15, 1.0597, 2.9922) 16.31
0.2	(6, 126, 2522)	(7, 113, 1212)	(8, 108, 782)	(8, 106, 605)	(9, 104, 447)
0.4	(3, 26, 623)	(3, 22, 242)	(3, 21, 143)	(3, 20, 107)	(3, 19, 78)
0.6	(2, 7, 86)	(2, 7, 38)	(2, 6, 26)	(2, 6, 22)	(2, 6, 18)
0.8	(2, 4, 17)	(2, 4, 11)	(2, 4, 10)	(2, 4, 9)	(2, 4, 9)
1.0	(1, 3, 7)	(2, 3, 7)	(2, 3, 7)	(2, 3, 6)	(2, 3, 6)
1.5	(1, 2, 3)	(1, 2, 4)	(1, 2, 4)	(1, 2, 4)	(1, 2, 4)
2.0	(1, 2, 2)	(1, 2, 3)	(1, 2, 3)	(1, 2, 3)	(1, 2, 3)
			$n = 7$		
	(3, 15, 1.0120, 3.1464) 16.07	(2, 15, 0.8857, 3.0775) 14.90	(2, 15, 0.8742, 3.0372) 14.20	(2, 15, 0.8683, 3.0153) 13.99	(2, 15, 0.8624, 2.9922) 13.69
0.2	(6, 106, 1562)	(6, 95, 852)	(7, 90, 586)	(7, 88, 470)	(7, 85, 366)
0.4	(2, 19, 298)	(3, 17, 140)	(3, 16, 93)	(3, 16, 75)	(3, 15, 60)
0.6	(2, 6, 42)	(2, 5, 24)	(2, 5, 19)	(2, 5, 17)	(2, 5, 15)
0.8	(2, 3, 11)	(2, 3, 8)	(2, 3, 7)	(2, 3, 7)	(2, 3, 7)
1.0	(1, 2, 5)	(1, 2, 5)	(1, 2, 5)	(1, 2, 4)	(1, 2, 4)
1.5	(1, 2, 3)	(1, 2, 3)	(1, 2, 3)	(1, 2, 3)	(1, 2, 3)
2.0	(1, 1, 2)	(1, 2, 2)	(1, 2, 2)	(1, 2, 2)	(1, 2, 2)
			$n = 9$		
	(4, 15, 0.7789, 3.1363) 14.15	(6, 15, 0.9858, 3.0712) 13.05	(5, 15, 0.8458, 3.0343) 12.49	(5, 15, 0.8403, 3.0139) 12.15	(5, 15, 0.8347, 2.9922) 11.81
0.2	(5, 92, 1151)	(6, 85, 673)	(6, 79, 478)	(6, 76, 393)	(6, 74, 317)

continue to next page

continue from previous page

0.4	(2, 16, 184)	(2, 15, 106)	(2, 14, 74)	(2, 14, 63)	(2, 13, 52)
0.6	(2, 5, 29)	(1, 5, 20)	(2, 4, 16)	(2, 4, 15)	(2, 4, 13)
0.8	(1, 3, 8)	(1, 2, 7)	(1, 2, 6)	(1, 2, 6)	(1, 2, 6)
1.0	(1, 2, 4)	(1, 2, 4)	(1, 2, 4)	(1, 2, 3)	(1, 2, 3)
1.5	(1, 2, 2)	(1, 1, 2)	(1, 1, 2)	(1, 1, 2)	(1, 1, 2)
2.0	(1, 1, 2)	(1, 1, 1)	(1, 1, 2)	(1, 1, 2)	(1, 1, 2)

TABLE 5. The optimal charting parameters (n_S, n_L, W, K) and the EMRL values of the VSS $\bar{X}$ chart, together with ($\ell_{0.05}$, MRL_1, $\ell_{0.95}$) values corresponding to specific shift sizes $\delta \in${0.2, 0.4, 0.6, 0.8, 1.0, 1.5, 2.0}, when $m \in${10, 20, 40, 80, $+\infty$}, $\text{MRL}_0 = 250$, $\text{ASS}_0 = n \in$ {3, 5, 7, 9} and $n_1 = n_L$

δ	$m = 10$ (n_S, n_L, W, K) EMRL ($\ell_{0.05}$, MRL_1, $\ell_{0.95}$)	$m = 20$ (n_S, n_L, W, K) EMRL ($\ell_{0.05}$, MRL_1, $\ell_{0.95}$)	$m = 40$ (n_S, n_L, W, K) EMRL ($\ell_{0.05}$, MRL_1, $\ell_{0.95}$)	$m = 80$ (n_S, n_L, W, K) EMRL ($\ell_{0.05}$, MRL_1, $\ell_{0.95}$)	$m = +\infty$ (n_S, n_L, W, K) EMRL ($\ell_{0.05}$, MRL_1, $\ell_{0.95}$)
			$n = 3$		
	(1, 15, 1.6357, 3.2029) 22.44	(1, 15, 1.5490, 3.1084) 20.72	(1, 15, 1.5099, 3.0542) 19.89	(1, 15, 1.4916, 3.0244) 19.44	(1, 15, 1.4740, 2.9922) 19.44
0.2	(2, 155, 7466)	(4, 146, 2499)	(6, 141, 1325)	(7, 139, 924)	(9, 138, 603)
0.4	(1, 40, 2733)	(1, 33, 755)	(1, 30, 352)	(1, 29, 225)	(1, 28, 132)
0.6	(1, 6, 484)	(1, 5, 121)	(1, 4, 57)	(1, 4, 38)	(1, 4, 26)
0.8	(1, 2, 60)	(1, 1, 19)	(1, 1, 11)	(1, 1, 8)	(1, 1,6)
1.0	(1, 1, 8)	(1, 1, 4)	(1, 1, 3)	(1, 1, 3)	(1, 1, 2)
1.5	(1, 1, 1)	(1, 1, 1)	(1, 1, 1)	(1, 1, 1)	(1, 1, 1)
2.0	(1, 1, 1)	(1, 1, 1)	(1, 1, 1)	(1, 1, 1)	(1, 1, 1)
			$n = 5$		
	(1, 15, 1.1450, 3.1660) 17.25	(1, 15, 1.1076, 3.0871) 15.98	(1, 15, 1.0895, 3.0422) 15.33	(1, 15, 1.0807, 3.0178) 14.90	(1, 15, 1.0720, 2.9922) 14.77
0.2	(3, 123, 2537)	(5, 113, 1220)	(6, 107, 787)	(6, 105, 609)	(7, 104, 450)
0.4	(1, 22, 608)	(1, 19, 244)	(1, 18, 142)	(1, 17, 105)	(1, 17, 76)
0.6	(1, 4, 80)	(1, 4, 35)	(1, 3, 23)	(1, 3, 19)	(1, 3, 15)
0.8	(1, 2, 13)	(1, 1, 8)	(1, 1, 6)	(1, 1, 5)	(1, 1, 5)
1.0	(1, 1, 4)	(1, 1, 3)	(1, 1, 3)	(1, 1, 2)	(1, 1, 2)
1.5	(1, 1, 1)	(1, 1, 1)	(1, 1, 1)	(1, 1, 1)	(1, 1, 1)
2.0	(1, 1, 1)	(1, 1, 1)	(1, 1, 1)	(1, 1, 1)	(1, 1, 1)
			$n = 7$		
	(1, 15, 0.8407, 3.1483) 14.72	(1, 15, 0.8174, 3.0777) 13.55	(1, 15, 0.8058, 3.0373) 12.98	(1, 15, 0.8001, 3.0153) 12.68	(1, 15, 0.7944, 2.9922) 12.38
0.2	(4, 103, 1561)	(5, 93, 850)	(5, 88, 583)	(6, 86, 468)	(6, 84, 363)
0.4	(1, 17, 285)	(1, 15, 136)	(1, 14, 90)	(1, 14, 72)	(1, 13, 57)

continue to next page

continue from previous page

0.6	(1, 4, 39)	(1, 3, 22)	(1, 3, 17)	(1, 3, 15)	(1, 3,13)
0.8	(1, 2, 9)	(1, 1, 6)	(1, 1, 5)	(1, 1, 5)	(1, 1, 5)
1.0	(1, 1, 3)	(1, 1, 3)	(1, 1, 3)	(1, 1, 2)	(1, 1, 2)
1.5	(1, 1, 1)	(1, 1, 1)	(1, 1, 1)	(1, 1, 1)	(1, 1, 1)
2.0	(1, 1, 1)	(1, 1, 1)	(1, 1, 1)	(1, 1, 1)	(1, 1, 1)
			$n = 9$		
	(1, 15, 0.5987, 3.1377) 13.19	(1, 15, 0.5832, 3.0723) 12.21	(1, 15, 0.5754, 3.0345) 11.56	(1, 15, 0.5716, 3.0140) 11.26	(1, 15, 0.5677, 2.9922) 11.01
0.2	(4, 90, 1147)	(5, 81, 661)	(5, 76, 469)	(5, 73, 384)	(5, 71, 308)
0.4	(1, 14, 177)	(1, 13, 96)	(1, 12, 69)	(1, 12, 58)	(1, 11, 49)
0.6	(1, 4, 27)	(1, 3, 18)	(1, 3, 14)	(1, 3, 13)	(1, 3, 12)
0.8	(1, 2, 7)	(1, 1, 6)	(1, 1, 5)	(1, 1, 5)	(1, 1, 4)
1.0	(1, 1, 3)	(1, 1, 3)	(1, 1, 2)	(1, 1, 2)	(1, 1, 2)
1.5	(1, 1, 1)	(1, 1, 1)	(1, 1, 1)	(1, 1, 1)	(1, 1, 1)
2.0	(1, 1, 1)	(1, 1, 1)	(1, 1, 1)	(1, 1, 1)	(1, 1, 1)

TABLE 6. Summary statistics of the Phase-I and Phase-II data obtained from the resistivity measurements (in Ω-cm) of silicon epitaxial wafers

Phase-I			Phase-II						
Subgroup number, i	$\bar{X}_i$	S_i	Subgroup number, i	$n_1 = n_S$			$n_1 = n_L$		
				n_i	$\bar{Y}_i$	$\hat{Z}_i$	n_i	$\bar{Y}_i$	$\hat{Z}_i$
1	4.4214	0.1106	21	6	4.4239	1.0087	15	4.3893	0.2575
2	4.3376	0.1214	22	15	4.4042	0.8343	8	4.4131	0.8595
3	4.4549	0.1236	23	6	4.3720	–0.2579	8	4.3660	–0.4682
4	4.3876	0.1425	24	6	4.3718	–0.2635	8	4.3839	0.0354
5	4.3753	0.1121	25	6	4.4196	0.9043	8	4.4189	1.0229
6	4.4164	0.0975	26	6	4.3291	–1.3069	8	4.3332	–1.3940
7	4.3550	0.1091	27	15	4.4163	1.3023	8	4.4041	0.6072
8	4.3302	0.0954	28	15	4.3844	0.0689	8	4.4128	0.8512
9	4.3202	0.0916	29	6	4.4037	0.5159	8	4.4433	1.7125
10	4.3167	0.0805	30	6	4.4796	2.3681	15	4.4916	**4.2098**
11	4.3890	0.0822	31	15	4.4983	**4.4659**	15	4.4983	**4.4659**
12	4.3467	0.0862	32	6	4.5180	**3.3057**	15	4.4795	**3.7426**
13	4.3501	0.1073	33	6	4.4832	2.4578	15	4.4845	**3.9346**
14	4.4626	0.0924	34	15	4.4516	2.6633	15	4.4516	2.6633
15	4.3039	0.1013	35	15	4.4663	**3.2323**	15	4.4663	**3.2323**
16	4.4505	0.1008							
17	4.4108	0.0876							
18	4.3701	0.0923							
19	4.4537	0.0821							
20	4.3992	0.0896							

The boldfaced values denote the out-of-control cases

Step 1 Specify the targeted values of τ, n, m, $n_{\max}$, $\delta_{\min}$, and $\delta_{\max}$.

Steps 2 and 3 Same as Steps 2 and 3 in the MRL optimisation model discussed in the previous section.

Step 4 Using the predetermined charting parameters (n_S, n_L, W, K) from Steps (2) and (3), evaluate the objective function EMRL using Equation (20). For solving the integral in Equation (20), the Gauss-Legendre Quadrature technique is adopted.

Step 5 Perform Steps 2 to 4 repeatedly to identify all the possible combinations of (n_S, n_L, W, K) for the VSS $\bar{X}$ chart using estimated process parameters when δ = 0, which satisfy constraints (16) - (18).

Step 6 Determine the optimal (n_S, n_L, W, K) combination for the VSS $\bar{X}$ chart using estimated process parameters that yields the most minimum EMRL value over a domain of mean shifts.

Through the aforementioned EMRL optimisation model, we can easily determine the optimal (n_S, n_L, W, K) parameters for the VSS $\bar{X}$ chart using estimated process parameters. In Tables 4 and 5, the optimal (n_S, n_L, W, K) parameters for the VSS $\bar{X}$ chart are shown for $m \in$ {10, 20, 40, 80, $+\infty$}, as well as the corresponding EMRL and ($\ell_{0.05}$, MRL_1, $\ell_{0.95}$) values, when $\delta \in$ {0.2, 0.4, 0.6, 0.8, 1.0, 1.5, 2.0}, $\mathrm{MRL}_0 = \tau$ = 250, and $\mathrm{ASS}_0 = n \in$ {3, 5, 7, 9}, for $n_1 = n_S$ and $n_1 = n_L$, respectively. For instance, under the condition of n = 3, m = 40, and $n_1 = n_L$, the VSS $\bar{X}$ chart is optimised with charting parameters (n_S, n_L, W, K) = (1, 15, 1.5099, 3.0542). These optimal parameters yield EMRL = 19.89 and ($\ell_{0.05}$, MRL_1, $\ell_{0.95}$) = (1, 4, 57) for δ = 0.6 (Table 5).

According to Tables 4 and 5, it is evident that, for any fixed n, an increase in the value of m leads to a reduction in the EMRL value, which tends to converge to the EMRL value when the process parameters are known ($m = +\infty$). For example, considering n = 5, and $n_1 = n_S$, the EMRL $\in$ {18.89, 17.39, 16.87, 16.48, 16.31} are obtained for the VSS $\bar{X}$ charts with $m \in$ {10, 20, 40, 80, $+\infty$}, respectively (Table 4). It is also apparent that as n increases, the EMRL value of the VSS $\bar{X}$ charts for both scenarios of estimated and known process parameters decreases. This suggests that increasing the value of n enhances the effectiveness and efficiency of the chart across a domain of shift sizes. Additionally, referring to Tables 4 and 5, we can recognise that the performance in detecting out-of-control conditions under the EMRL optimisation model is nearly identical to that under the MRL optimisation model, as shown in Tables 2 and 3. For illustration, when n = 9, m = 10, and δ_{opt} = 0.2, we obtain ($\ell_{0.05}$, MRL_1, $\ell_{0.95}$) = (4, 90, 1149) for the optimal MRL-based VSS $\bar{X}$ chart (Table 3), while the optimal EMRL-based VSS $\bar{X}$ chart has ($\ell_{0.05}$, MRL_1, $\ell_{0.95}$) = (4, 90, 1147) (Table 5). Thus, it is suggested to employ the optimal EMRL-based VSS $\bar{X}$ chart using estimated process parameters, as it exhibits equal or superior performance compared to the optimal MRL-based VSS $\bar{X}$ chart, especially in practical scenarios where shift sizes are typically unknown and difficult to predict.

A REAL-LIFE DATA APPLICATION

Within this section, real-life data provided by a wafer substrate manufacturing firm is adopted to showcase the operation of the proposed optimal VSS $\bar{X}$ charts. The VSS $\bar{X}$ charts demonstrated in this section employ the MRL metric and estimated process parameters. The dataset includes information on the epitaxial processing of silicon wafers used in the semiconductor sector. Serving as the fundamental material for creating integrated circuits and semiconductor devices, silicon epitaxial wafers are essential for the functionality of today's electronic technology. These wafers consist of monocrystalline layers deposited onto substrates and are commonly manufactured with varying resistivities (measured in ohm-centimetre, Ω-cm). Monitoring the resistivity of the silicon epitaxial wafer is vital for maintaining the high-quality production of electronic devices, ultimately enhancing their longevity and efficiency. Therefore, the individual resistivity measurement of silicon epitaxial wafers is identified as the key quality characteristic of interest for this application example.

The raw data for the resistivity measurements of silicon epitaxial wafers are collected from 35 samples. The first 20 samples (Phase-I) are used to configure the proposed optimal VSS $\bar{X}$ chart, with the subsequent 15 samples (Phase-II) applied to analyse the effectiveness and efficiency of the proposed optimal control chart. The detailed summary statistics for the resistivity measurements of silicon epitaxial wafers in both Phase-I and Phase-II are given in Table 6. Assuming an MRL_0 of 250, the monitoring schemes in this analysis is optimised to detect a shift of δ_{opt} = 0.8.

During the Phase-I calibration stage, a dataset consisting of m = 20 individual resistivity measurements is collected, each with a sample size n = 9. First, Ryan's (2000) Bonferroni-type adjustment is employed to analyse the stability of the data gathered in Phase-I. The calculation of control limits for the Bonferroni-adjusted $\bar{X}$ and S charts is determined through $UCL_{\bar{X}}/LCL_{\bar{X}} = \bar{\bar{X}} \pm Z_{FAP/(2m)}(\bar{S}/c_4)/\sqrt{n}$ and $UCL_S/LCL_S = \bar{S} \pm Z_{FAP/(2m)}\sqrt{1-c_4^2}(\bar{S}/c_4)$, respectively. Here, $\bar{\bar{X}}$ = 4.3826 refers to the grand average of samples, $\bar{S}$ = 0.1003 denotes the average standard deviation across m samples, Z_ς represents the $(1-\varsigma)\times 100^{\mathrm{th}}$ percentile of the standard normal distribution, $c_4 = \sqrt{2/(n-1)}(\Gamma(n/2)/\Gamma((n-1)/2))$ = 0.9693 (Ryan 2000) indicates a fixed constant that remains unbiased, and FAP = 0.0834 signifies the probability of encountering a

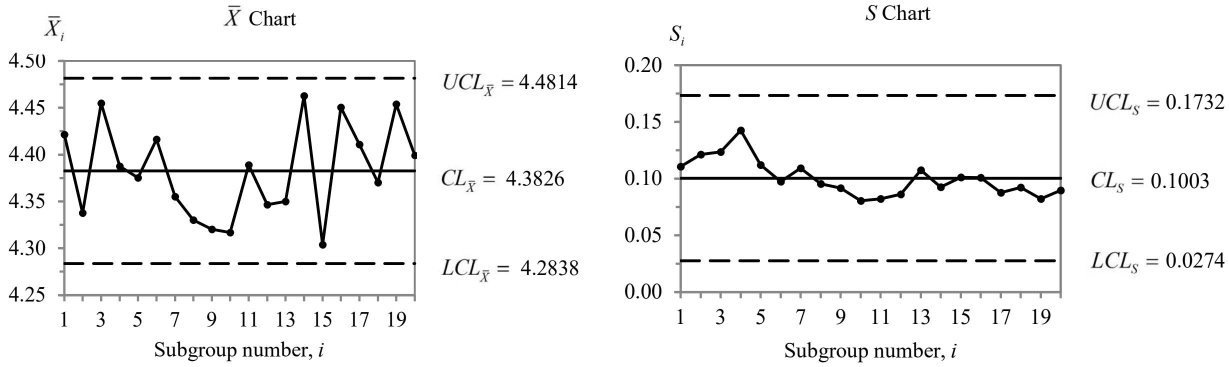

(a) (b)

FIGURE 3. An analysis of the Bonferroni-adjusted (a) $\bar{X}$ and (b) S charts for evaluating the Phase-I data

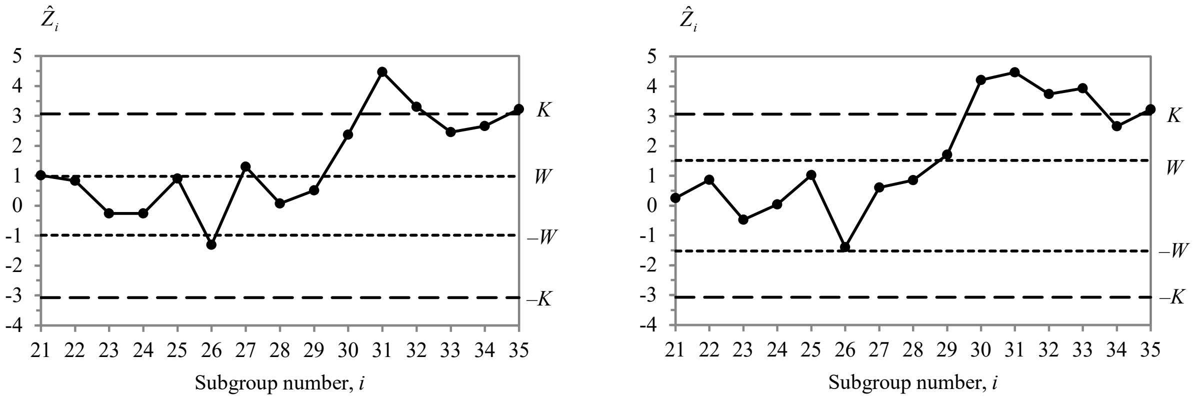

(a) (b)

FIGURE 4. The VSS $\bar{X}$ chart with estimated process parameters for monitoring the Phase-II data when (a) $n_1 = n_S$ and (b) $n_1 = n_L$

false alarm. Note that $\Gamma(\cdot)$ represents the gamma function. Using Equation (10), the corresponding ARL_0 = 459.64 (equivalent to MRL_0 = 250) is computed with m = 20, δ_{opt} = 0.8, and n = 9, based on the optimal charting parameters (n_S, n_L, W, K) = (6, 15, 0.9858, 3.0712) for $n_1 = n_S$ (Table 2). Given ARL_0 = 459.64, a false alarm is expected to occur at each sampling point with a probability of 0.002176. As a result, the probability of encountering a false alarm occurring at least once over 40 sampling points is calculated as FAP = $1-(1-0.002176)^{40} = 0.0834$. Figure 3 provides the complete evaluation of the Phase-I data through the Bonferroni-adjusted $\bar{X}$ and S charts. Based on Figure 3, it indicates that the Phase-I data is operating under the in-control conditions. Then, the estimated in-control mean $\hat{\mu}_0 = 4.3826$ Ω-cm, and standard deviation $\hat{\sigma}_0 = 0.1003$ Ω-cm are calculated by employing Equations (1) and (2), respectively.

In Phase-II process monitoring, the optimal charting parameters for the VSS $\bar{X}$ charts based on estimated process parameters are found to be (n_S, n_L, W, K) = (6, 15, 0.9858, 3.0712) (Table 2) and (8, 15, 1.5196, 3.0703) (Table 3) for $n_1 = n_S$ and $n_1 = n_L$, respectively, when MRL_0 = 250, m = 20, n = 9, and δ_{opt} = 0.8. The optimal VSS $\bar{X}$ chart, based on estimated process parameters, is shown in Figure 4 for monitoring the Phase-II resistivity measurements when $n_1 = n_S$ and $n_1 = n_L$. To provide a comprehensive understanding of the operational mechanism for the optimal VSS $\bar{X}$ chart for $n_1 = n_S$ and $n_1 = n_L$ in this application, we offer the following explanations. When using the optimal VSS $\bar{X}$ chart with $n_1 = n_S$ = 6, the first $\bar{Y}_{21}$ = 4.4239 is calculated based on $n_{21} = n_S$ = 6 measurements, and its corresponding $\hat{Z}_{21}$ = 1.0087 is computed using Equation (3). Note that n_{21} in this example is the first subgroup (n_1) in Phase-II process monitoring. Since $\hat{Z}_{21}$ falls within (W, K], the next sample $\bar{Y}_{22}$ is collected and calculated using $n_{22} = n_L = 15$. The corresponding $\hat{Z}_{22} = 0.8343$ is computed, which lies within [–*W*, *W*]. Subsequently, $n_{23} = n_S = 6$ is used to calculate the next sample $\bar{Y}_{23} = 4.3720$ with the respective $\hat{Z}_{23} = -0.2579$. This process continues until sample $\bar{Y}_{31} = 4.4983$, where $\hat{Z}_{31} = 4.4659$ falls within (*K*, $+\infty$). At this point, the optimal VSS $\bar{X}$ chart with $n_1 = n_S$ produces the first out-of-control signal at the 31st subgroup (Figure 4(a) and the boldfaced values in Table 6). Other out-of-control samples are detected by the chart at 32nd and 35th subgroups.

In a similar manner, when employing the optimal VSS $\bar{X}$ chart with $n_1 = n_L = 15$, the first $\bar{Y}_{21} = 4.3893$ in Phase-II process monitoring, is computed using n_L=15 collected measurements. As its respective $\hat{Z}_{21}$ 0.2575 falls within [–*W*, *W*], the subsequent sample $\bar{Y}_{22}$ is collected and calculated as 4.4131 using $n_{22} = n_S = 8$. The corresponding $\hat{Z}_{22}$ is then determined to be 0.8595. This process continues until sample $\bar{Y}_{30} = 4.4916$, where $\hat{Z}_{30} = 4.2098$ is located within (*K*, $+\infty$). At this stage, the optimal VSS $\bar{X}$ chart with $n_1 = n_L$ immediately generates the first out-of-control condition at 30th subgroup. The remaining out-of-control points are detected at the 31st – 33rd and 35th subgroups (Figure 4(b) and the boldfaced values in Table 6). Once the out-of-control cases are successfully detected, appropriate and immediate investigations are conducted to determine and omit the assignable cause(s).

Notably, the optimal MRL-based VSS $\bar{X}$ chart using estimated process parameters for $n_1 = n_L$ signals an out-of-control sample more quickly than the corresponding VSS $\bar{X}$ chart with $n_1 = n_S$. This observation indicates that opting for a larger sample size in the first subgroup can enhance the detection capabilities of the VSS $\bar{X}$ chart using estimated process parameters.

CONCLUSIONS

Current SPC literature predominantly emphasises on the ARL criterion for optimising control charts, which may lead to overlooking some important aspects of the control chart's overall effectiveness. This is absolutely true as we show that the ARL-based VSS $\bar{X}$ chart, when process parameters are estimated, results in high false alarm rates and significantly increased operational costs. Therefore, we argue that the ARL metric is a misleading measure when applying to control charts using estimated process parameters for practitioners due to economical and operational reasons. This paper introduces theoretical frameworks for designing the VSS $\bar{X}$ chart using estimated process parameters, with an emphasis on the MRL and other percentiles of the run-length distribution, such as $\ell_{0.05}$, $\ell_{0.25}$, $\ell_{0.75}$, and $\ell_{0.95}$. These percentiles provide more useful information and practical benefits for practitioners in industrial settings. Two new optimal statistical designs for the VSS $\bar{X}$ charts using estimated process parameters are implemented by minimising the MRL_1 and EMRL metrics for known and unknown shift-size conditions, respectively. These designs consider two schemes, where $n_1 = n_S$ and $n_1 = n_L$. The EMRL criterion is evaluated for its ability to address the random shift-size issue, which is commonly encountered in practical environments.

Moreover, Tables 2 to 5 provide ready-to-used optimal charting parameters for the proposed VSS $\bar{X}$ chart using estimated process parameters, tailored to various choices of Phase-I samples *m*. The intention of these tables is to facilitate and support practitioners in the practical implementation of the proposed charts. Our findings indicate that, when estimating process parameters, the MRL-based and EMRL-based VSS $\bar{X}$ charts produce a minimised false alarm rate and offer simpler interpretations for practitioners in analysing the behaviour of the run-length distribution, compared to the VSS $\bar{X}$ chart designed using the ARL criterion. From the SPC perspective, a reduced false alarm rate is preferable for the proposed optimal VSS $\bar{X}$ chart using estimated process parameters. The rationale is that it reliably guarantees better resource management for manufacturers, such as avoiding unnecessary time spent to investigate non-existent root causes in the process. Furthermore, to attain comparable detection capability to that of the scenario with known process parameters, practitioners are advised to select $m \geq 80$ for the proposed VSS $\bar{X}$ chart under the scenario of estimated process parameters. Additionally, the associated sampling costs should be considered in this selection process. An application using the resistivity measurements of silicon epitaxial wafers, is employed to demonstrate the practicality and reliability of the MRL-optimised VSS $\bar{X}$ chart in real-world situations when estimating process parameters.

For future research directions, researchers are encouraged to explore the MRL- and EMRL- optimised VSI $\bar{X}$ chart using estimated process parameters. The VSI scheme offers dynamic adaptability, enabling real-time adjustments to sampling frequency based on process behaviour, thereby improving the responsiveness and accuracy of process monitoring. Alternatively, examining the influences of parameter estimation on the performance of the VSS median chart, along with utilising MRL and EMRL metrics could be another valuable avenue for future investigation. The median offers a more reliable measure of central tendency in control chart settings, especially with skewed distributions or outliers.

ACKNOWLEDGEMENTS

This research was supported and funded by the Ministry of Higher Education (MOHE), Malaysia under the Fundamental Research Grant Scheme (FRGS), No. FRGS/1/2021/STG06/HWUM/02/1.

REFERENCES

Castagliola, P., Maravelakis, P.E. & Figueiredo, F.O. 2016. The EWMA median chart with estimated parameters. *IIE Transactions* 48(1): 66-74.

Castagliola, P., Zhang, Y., Costa, A. & Maravelakis, P. 2012. The variable sample size $\bar{X}$ chart with estimated parameters. *Quality and Reliability Engineering International* 28(7): 687-699.

Chakraborti, S. 2007. Run length distribution and percentiles: The Shewhart $\bar{X}$ chart with unknown parameters. *Quality Engineering* 19(2): 119-127.

Chong, Z.L., Tan, K.L., Khoo, M.B.C., Teoh, W.L. & Castagliola, P. 2022. Optimal designs of the exponentially weighted moving average (EWMA) median chart for known and estimated parameters based on median run length. *Communications in Statistics – Simulation and Computation* 51(7): 3660-3684.

Chong, Z.L., Yeong, W.C., Khaw, K.W., Chew, X.Y. & Teoh, W.L. 2024. Optimal design of the side sensitive group runs double sampling (SSGRDS) $\bar{X}$ scheme with estimated process parameters. *Transactions of the Institute of Measurement and Control* 47(3): 487-505.

Costa, A.F.B. 1994. $\bar{X}$ charts with variable sample size. *Journal of Quality Technology* 26(3): 155-163.

Epprecht, E.K., Loureiro, L.D. & Chakraborti, S. 2015. Effect of the amount of phase I data on the phase II performance of S^2 and S control charts. *Journal of Quality Technology* 47(2): 139-155.

Gan, F.F. 1993. An optimal design of EWMA control charts based on median run length. *Journal of Statistical Computation and Simulation* 45(3-4): 169-184.

Gao, H., Khoo, M.B.C., Teh, S.Y. & Teoh, W.L. 2019. A study on the median run length performance of the run sum S control chart. *International Journal of Mechanical Engineering and Robotics Research* 8(6): 885-890.

Hu, X.L., Castagliola, P., Sun, J.S. & Khoo, M.B.C. 2016. The performance of variable sample size $\bar{X}$ chart with measurement errors. *Quality and Reliability Engineering International* 32(3): 969-983.

Jensen, W.A., Jones-Farmer, L.A., Champ, C.W. & Woodall, W.H. 2006. Effects of parameter estimation on control chart properties: A literature review. *Journal of Quality Technology* 38(4): 349-364.

Karimi, H., Khaw, K.W., Chew, X.Y., Chong, Z.L. & Lim, S.T. 2023. Variable sample size control charts for monitoring multivariate coefficient of variation based on median run length and expected median run length. *Journal of Science and Technology* 15(2): 54-80.

Lee, M.H., Khoo, M.B.C., Haq, A., Wong, D.M.L. & Chew, X.Y. 2023. Synthetic *c* charts with known and estimated process parameters based on median run length and expected median run length. *Quality Technology & Quantitative Management* 20(2): 168-183.

Lim, S.L., Yeong, W.C., Chong, Z.L., Gan, C.P. & Khoo, M.B.C. 2024. A variable sample size side-sensitive synthetic coefficient of variation chart. *Transactions of the Institute of Measurement and Control* 46(9): 1694-1712.

Montgomery, D.C. 2013. *Statistical Quality Control: A Modern Introduction*. 7th ed. New York: John Wiley & Sons.

Mim, F.N., Khoo, M.B.C., Saha, S. & Castagliola, P. 2022. Revised triple sampling $\bar{X}$ control charts for the mean with known and estimated process parameters. *International Journal of Production Research* 60(16): 4911-4935.

Qiao, Y.L., Sun, J.S., Castagliola, P. & Hu, X.L. 2022. Optimal design of one-sided exponential EWMA charts based on median run length and expected median run length. *Communications in Statistics - Theory and Method* 51(9): 2887-2907.

Reynolds Jr., M.R. 1996. Variable-sampling-interval control charts with sampling at fixed times. *IIE Transactions* 28(6): 497-510.

Ryan, T.P. 2000. *Statistical Methods for Quality Improvement.* 2nd ed. New York: John Wiley & Sons.

Shepherd, D.K., Champ, C.W. & Rigdon, S.E. 2016. Properties of the Markov-dependent attribute control chart with estimated parameters. *Quality and Reliability Engineering International* 32(2): 485-498.

Teh, S.Y., Khoo, M.B.C., Ong, K.H., Soh, K.L. & Teoh, W.L. 2015. A study on the S^2-EWMA chart for monitoring the process variance based on the MRL performance. *Sains Malaysiana* 44(7): 1067-1075.

Teoh, J.W., Teoh, W.L., Khoo, M.B.C., Tran, K.P. & Lee, M.H. 2024. An integrated optimal-GICP design for the SPRT control chart with estimated process parameters based on the average number of observations to signal. *Quality Technology & Quantitative Management* 22(1): 84-104.

Teoh, W.L., Chong, J.K., Khoo, M.B.C., Castagliola, P. & Yeong, W.C. 2017. Optimal designs of the variable sample size $\bar{X}$ chart based on median run length and expected median run length. *Quality and Reliability Engineering International* 33(1): 121-134.

Teoh, W.L., Khoo, M.B.C., Castagliola, P. & Lee, M.H. 2016. The exact run length distribution and design of the Shewhart $\bar{X}$ chart with estimated parameters based on median run length. *Communications in Statistics – Simulation and Computation* 45(6): 2081-2103.

Teoh, W.L., Khoo, M.B.C., Castagliola, P. & Chakraborti, S. 2015. A median run length-based double sampling $\bar{X}$ chart with estimated parameters for minimizing the average sample size. *The International Journal of Advanced Manufacturing Technology* 80(1-4): 411-426.

Teoh, W.L., Khoo, M.B.C., Castagliola, P. & Chakraborti. S. 2014. Optimal designs of the double sampling $\bar{X}$ chart with estimated parameters based on median run length. *Computers & Industrial Engineering* 67(1): 104-115.

Yeong, W.C., Tan, Y.Y., Lim, S.L., Khaw, K.W. & Khoo, M.B.C. 2022. A variable sample size run sum coefficient of variation chart. *Quality and Reliability Engineering International* 38(4): 1869-1885.

You, H.W., Khoo, M.B.C., Castagliola, P. & Qu, L. 2016. Optimal exponentially weighted moving average charts with estimated parameters based on median run length and expected median run length. *International Journal of Production Research* 54(17): 5073-5094.

Zhou, Q., Zou, C., Wang, Z. & Jiang, W. 2012. Likelihood-based EWMA charts for monitoring Poisson count data with time-varying sample sizes. *Journal of the American Statistical Association* 107(499): 1049-1062.

*Corresponding author; email: wei_lin.teoh@hw.ac.uk